

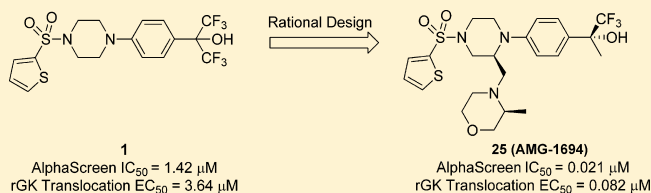
# Small Molecule Disruptors of the Glucokinase–Glucokinase Regulatory Protein Interaction: 1. Discovery of a Novel Tool Compound for in Vivo Proof-of-Concept

Kate S. Ashton,<sup>\*,†</sup> Kristin L. Andrews,<sup>‡</sup> Marion C. Bryan,<sup>†,▽</sup> Jie Chen,<sup>⊥</sup> Kui Chen,<sup>‡</sup> Michelle Chen,<sup>||</sup> Samer Chmait,<sup>‡</sup> Michael Croghan,<sup>†</sup> Rod Cupples,<sup>||</sup> Christopher Fotsch,<sup>†</sup> Joan Helmering,<sup>||</sup> Steve R. Jordan,<sup>‡</sup> Robert J. M. Kurzeja,<sup>§</sup> Klaus Michelsen,<sup>‡</sup> Lewis D. Pennington,<sup>†</sup> Steve F. Poon,<sup>†</sup> Glenn Sivits,<sup>||</sup> Gwyneth Van,<sup>#</sup> Steve L. Vonderfecht,<sup>#,○</sup> Robert C. Wahl,<sup>†</sup> Jiandong Zhang,<sup>‡,◆</sup> David J. Lloyd,<sup>||</sup> Clarence Hale,<sup>||</sup> and David J. St. Jean, Jr.<sup>†</sup>

<sup>†</sup>Department of Therapeutic Discovery—Medicinal Chemistry, <sup>‡</sup>Department of Therapeutic Discovery—Molecular Structure and Characterization, <sup>§</sup>Department of Therapeutic Discovery—Protein Technologies, <sup>||</sup>Department of Metabolic Disorders, <sup>⊥</sup>Department of Pharmacokinetics and Drug Metabolism, <sup>#</sup>Department of Pathology, Amgen, Inc., One Amgen Center Drive, Thousand Oaks, California 91320-1799, United States

## Supporting Information

**ABSTRACT:** Small molecule activators of glucokinase have shown robust efficacy in both preclinical models and humans. However, overactivation of glucokinase (GK) can cause excessive glucose turnover, leading to hypoglycemia. To circumvent this adverse side effect, we chose to modulate GK activity by targeting the endogenous inhibitor of GK, glucokinase regulatory protein (GKRP). Disrupting the GK–GKRP complex results in an increase in the amount of unbound cytosolic GK without altering the inherent kinetics of the enzyme. Herein we report the identification of compounds that efficiently disrupt the GK–GKRP interaction via a previously unknown binding pocket. Using a structure-based approach, the potency of the initial hit was improved to provide **25** (AMG-1694). When dosed in ZDF rats, **25** showed both a robust pharmacodynamic effect as well as a statistically significant reduction in glucose. Additionally, hypoglycemia was not observed in either the hyperglycemic or normal rats.



## INTRODUCTION

Glucokinase (GK) is an enzyme in the hexokinase family that converts glucose to glucose-6-phosphate (G6P).<sup>1</sup> GK plays a key role in maintaining glucose homeostasis as it facilitates glucose entry into the glycolytic pathway in the liver and also regulates G6P levels in pancreatic  $\beta$ -cells.<sup>2</sup> Allosteric activation of GK with small molecules has been shown to lower blood glucose levels in both rodent models of diabetes and type 2 diabetics.<sup>3–5</sup> One potential disadvantage of GK activators (GKAs), that has manifested in the clinic, is hypoglycemia caused by overactivation of GK.<sup>6,7</sup> Indeed, many recent reviews have highlighted this shortcoming and have begun to question the legitimacy of targeting GK as a chronic treatment for diabetes.<sup>8,9</sup> However, the robust efficacy exhibited by GKAs<sup>10</sup> provided compelling evidence to investigate novel ways to target the glucose phosphorylation pathway.

In hepatocytes, GK activity is partially controlled by the glucokinase regulatory protein (GKRP). The primary role of GKRP is to sequester GK in the nucleus during fasting.<sup>11</sup> The GK–GKRP complex is glucose dependent, and a postprandial rise in blood sugar results in disruption of the complex. The unbound GK then translocates to the cytoplasm where it facilitates glucose metabolism.<sup>12,13</sup> By targeting this protein–

protein interaction, the native kinetics of GK would remain unchanged,<sup>14</sup> and therefore, the risk of hypoglycemia could potentially be lowered. Also, because GKRP is expressed almost exclusively in the liver,<sup>15</sup> disrupting the GK–GKRP complex would result in an increase in the amount of active hepatic GK. As such, pancreatic effects would not be observed, and the increased insulin secretion seen with GKAs could be avoided.<sup>16</sup>

## RESULTS AND DISCUSSION

To identify a compound that acted upon the GK–GKRP complex selectively (i.e., no GK activation), a high throughput screen (HTS) was conducted that measured the increase of glucose phosphorylation in the presence of both GK and GKRP.<sup>17</sup> The hits from this screen were then counter-screened in the presence of GK only. Those compounds that were effective in the GK–GKRP assay, but had no activity in the GK only assay, were considered for further evaluation. To fully characterize the activity of these analogues, a binding and a functional assay were developed. An AlphaScreen assay (bead-based proximity assay) was established utilizing fluorescein

Received: October 28, 2013

tagged GK and biotinylated AviTag GGRP. The potency of a compound (the ability to disrupt the GK-GGRP complex) was directly related to the intensity of the fluorescence signal. The functional assay was developed using freshly harvested rat hepatocytes. The plated cells were treated with test compounds, and GK was visualized with a fluorescently labeled secondary antibody.<sup>18</sup> The difference between the average intensity of nuclear GK minus the average intensity of cytoplasmic (or active) GK was then quantified using an Operetta platform.

A confirmed GK-GGRP disruptor was identified and displayed an AlphaScreen IC<sub>50</sub> of 1.42  $\mu$ M (Figure 1).<sup>19</sup> The

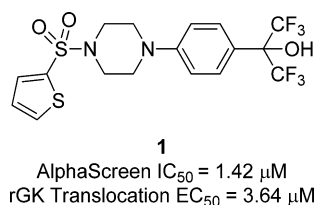


Figure 1. Initial HTS hit.

hit (1) also demonstrated modest cellular activity in the rat hepatocyte assay (3.64  $\mu$ M). An X-ray co-crystal structure of 1 with hGGRP was obtained. Analysis of the structure revealed that 1 bound to GGRP in a previously unknown, well-defined binding pocket distinct from the sugar binding region (Figure 2).<sup>20–22</sup>

Key interactions of compound 1 with GGRP are highlighted in Figure 3. The sulfonamide on compound 1 provided the trajectory needed to direct the thiophene into a “left hand” pocket comprised of residues Arg215 and Ala214. The aryl ring

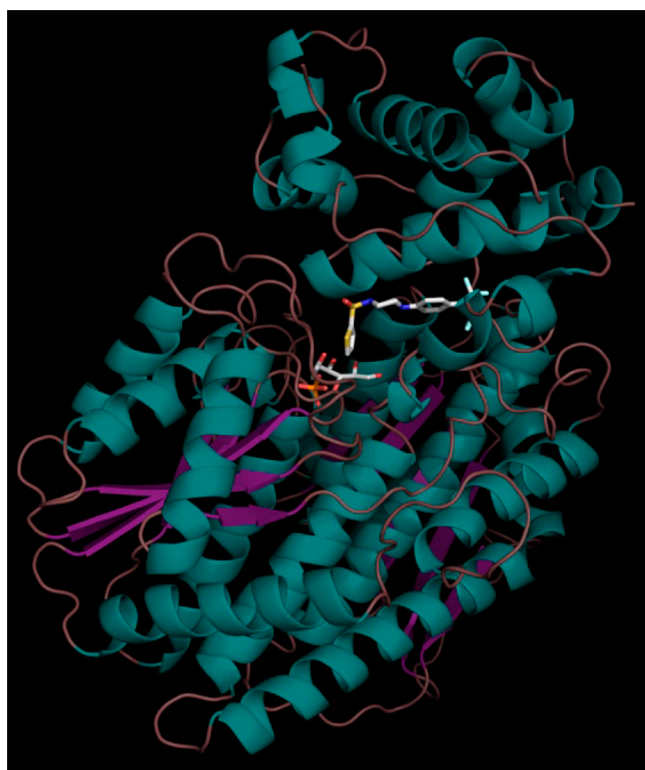


Figure 2. X-ray co-crystal structure of HTS hit 1 and sorbitol-6-phosphate (both shown in white) bound to hGGRP.

was positioned so that it navigated a tight hydrophobic channel, forming van der Waals contacts with Ala521 above and Val28 and Glu32 below. The tertiary hydroxyl group on compound 1 formed a hydrogen bond with the side chain guanidine of Arg525. This hydrophilic residue facilitated incorporation of polarity into the molecule and the surrounding hydrophobic region accommodated the bulky trifluoromethyl groups. Situated 4 Å from the SO<sub>2</sub> moiety is the side chain of Arg215 which, although not engaged in a formal hydrogen bond, likely interacts in a favorable electrostatic manner.

The simplicity of the molecule and its reasonable binding efficiency (BE = 0.30)<sup>23</sup> made it an attractive starting point for optimization. Because GK-GGRP disruption as a means to lower blood glucose in preclinical animal models had not been reported, the initial goal was to identify a GK-GGRP inhibitor that could be tested in a rat disease model (e.g., Zucker Diabetic Fatty (ZDF) rats). Toward this end, we desired a compound that was at least 100-fold more potent than 1 and had in vivo PK properties suitable for oral dosing. Unfortunately, the pharmacokinetics of 1 (Table 1) indicated that the unbound plasma concentration would be unable to reach the EC<sub>50</sub> in vivo at a reasonable dose (below 100 mg/kg). Herein we report the optimization of 1 with a focus on improving potency as a means toward achieving a tool compound for proof-of-concept in vivo experiments.

Initial SAR studies relied on the co-crystal structure of 1 bound to hGGRP. It was apparent from the crystal structure that there was a hydrophobic pocket above the piperazine ring (shown in Figure 3) and that this area could be accessed via an axial substituent on the piperazine.<sup>24</sup> Table 2 shows our initial efforts at potency optimization through piperazine substitution. Compound 3 confirmed that a (*S*)-methyl substituent was tolerated (cf. (*R*)-methyl in 2) and that the positioning was critical to potency. The analogues with the methyl group positioned next to the sulfonamide nitrogen (compounds 4 and 5) were 10-fold less active. Larger groups were accommodated; however, no gains in potency were obtained with the ethyl, isopropyl, and aryl derivatives (6–8). The benzyl analogue (9) modeled well, with good complementarity to the pocket, and a modest increase in potency was observed relative to 1. Further substitution of the aromatic ring, however, resulted in no significant gains in activity (10–15).

Simply adding lipophilic groups at the piperazine C-3 position to maximize van der Waals contacts had so far not proven successful at improving potency. The “top” pocket of GGRP contained many neutral residues and was hydrophobic in nature, although the N–H of Ile11 pointed directly toward the center of this region (Figure 4). To try to capitalize on this interaction, an H-bond acceptor was incorporated in the form of a pyridine (16). This analogue was not as potent as compound 9, and we hypothesized that the pyridine analogue did not possess the correct geometry to optimally satisfy the Ile11 hydrogen bond donor. Incorporation of an H-bond acceptor in the form of a 4-tetrahydropyranyl (THP) group (18) was designed as an alternative to satisfy the NH on Ile11. Relative to cyclohexyl analogue 17, the THP analogue showed a >25-fold increase in biochemical activity, suggesting that the orientation of the H-bond acceptor now engaged Ile11. The morpholine analogue, 19, which also contained a hydrogen-bond accepting oxygen, had an IC<sub>50</sub> similar to THP analogue 18. Both of these compounds showed weak activity in the translocation assay (EC<sub>50</sub> values for 18 and 19 were 5.47 and 3.99  $\mu$ M, respectively), and we rationalized that an order of

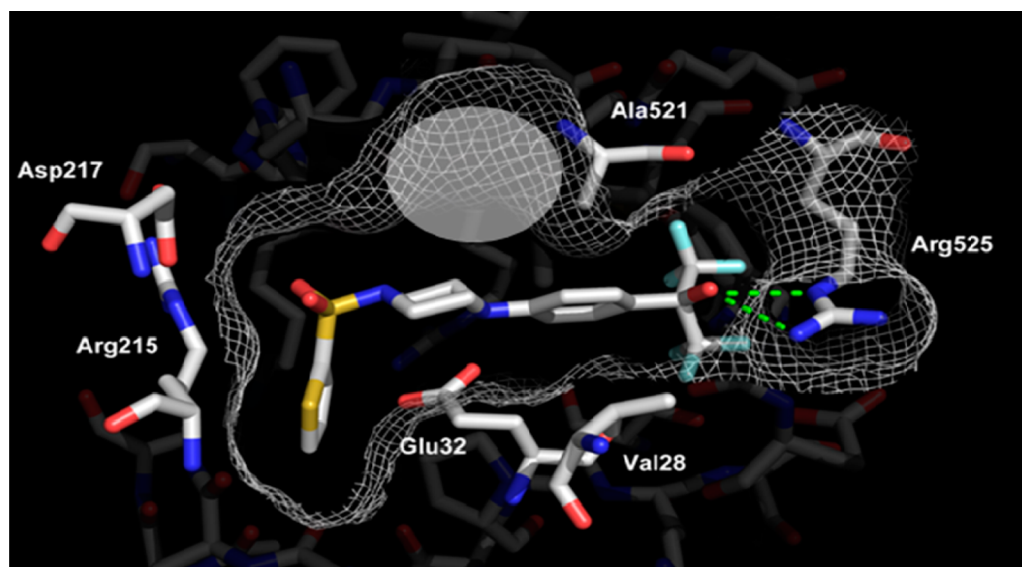


**Figure 3.** The X-ray co-crystal structures of **1** (white) with hGKR. The key hydrogen bonding interactions are shown with green dashed lines, the surface area of the binding site is represented by gray mesh, and the targeted pocket is highlighted by a gray oval.

**Table 1. Activity and Rat in Vivo PK Properties of HTS Hit 1**

compd	rGK translocation EC <sub>50</sub> <sup>a</sup> (μM)	RLM CL <sub>int</sub> <sup>b</sup> (μL/min/mg)	CL <sup>c</sup> (L/h/kg)	V <sub>ss</sub> <sup>c</sup> (L/kg)	C <sub>max</sub> <sup>d</sup> (μM)	F <sup>d</sup> (%)	f <sub>u</sub> <sup>e</sup> (%)
<b>1</b>	3.64	150	2.64	6.81	0.35	28	0.62

<sup>a</sup>Data reported as the mean where  $n \geq 3$ , standard deviation reported in the Supporting Information <sup>b</sup>In vitro microsomal stability measurements were conducted in the presence of NADPH at 37 °C for 30 min at a final compound concentration of 1 μM. <sup>c</sup>2 mg/kg intravenous dose (100% DMSO). <sup>d</sup>10 mg/kg oral dose (0.1% Tween 80, 0.5% CMC, 99.4% water). <sup>e</sup>Fraction unbound, determined via rapid equilibrium dialysis.

magnitude increase in biochemical potency was still required to make these molecules useful in vivo tool compounds.<sup>25</sup> On the basis of the model of compound **19** in the GKR binding site (Figure 4), we identified a small hydrophobic pocket positioned directly above the 2-position of the morpholine (Figure 4). In an attempt to increase the biochemical potency of **19** by occupying this small subpocket, an axial methyl group was incorporated.

In the case of *N*-substituted morpholines, the lowest energy conformation for a methyl group at the 3-position is axial.<sup>26</sup> Gratifyingly, analogue **20** showed improved potency and had a 4-fold increase in IC<sub>50</sub> relative to the parent analogue **19**. Unfortunately, this did not translate into lower cellular potency because the translocation assay showed little improvement over **1** (1.81 μM in rat primary hepatocytes for **20**).

Having optimized the van der Waals and hydrogen bonding contacts with the hydrophobic pockets, we next turned to modifying the physiochemical properties of the compound in an attempt to improve cellular potency. The first of these changes was substitution of one of the trifluoromethyl groups adjacent to the tertiary hydroxyl with a methyl moiety. This was an attempt to reduce the lipophilicity of the molecule and potentially improve its cell potency.<sup>27</sup> The cLogP values of the methyl/trifluoromethyl analogues (**21** and **22**) were lower in both the THP and the methyl morpholine case versus their corresponding hexafluoro analogues (**18** and **20**) (Table 3). Although the IC<sub>50</sub> values for **23** and **24** remained similar to the hexafluoro analogue **18**, the hepatocyte EC<sub>50</sub> value for enantiomer **23** was around 6-fold more potent than compound **18** (0.89 and 5.47 μM, respectively, Table 4). In the case of the methyl morpholine derivatives (**25** (AMG-1694)<sup>22</sup> and **26**), the cellular EC<sub>50</sub> value of the (*R*)-enantiomer (**25**) demonstrated a

20-fold improvement over its hexafluoro analogue (0.082 vs 1.81 μM for **20**).

Interestingly the compounds with a (*R*)-configuration at the hydroxyl stereocenter exhibited better cellular potencies than their (*S*)-analogues in both of the head to head comparisons of **23** to **24** and **25** to **26**. The X-ray crystal structure of **25** (Figure 5) showed that the compound bound as predicted with key hydrogen bonding interaction with both Ile11 and Arg525.

Since the potent cellular activity of the methyl-morpholine analogue **25** was encouraging, its pharmacokinetic properties were evaluated. Despite its high in vivo clearance, the rat PK suggested that we could approach the EC<sub>50</sub> value in vivo at a 100 mg/kg dose (Table 5).<sup>28</sup>

Several methods were developed for the synthesis of the 2-substituted piperazines, the general schemes shown allowed facile access to all of the fully elaborated compounds. Shown in Scheme 1 is the synthesis used for the compounds which involved substituted piperazines that were available commercially.

The majority of the starting material piperazines were procured as monoprotected Boc derivatives, and the synthesis of the final compounds involved arylation via a palladium mediated coupling and removal of the Boc group followed by sulfonylation (**1–3**, **6**, and **9**). When the unprotected piperazine was available, the sequence was reversed and the material sulfonylated prior to arylation (**7**). Both the sulfonylated and Boc protected piperazines worked well in the cross-coupling reaction with aryl bromides. For synthesis of the piperazines with a substituent adjacent to the sulfonamide, the unprotected piperazine was used and arylation was selective for the less hindered nitrogen (**4** and **5**). Scheme 2 outlines the

Table 2. Piperazine Substituent SAR

Cmpd	Structure	AlphaScreen IC <sub>50</sub> <sup>a</sup> (μM)	Cmpd	Structure	AlphaScreen IC <sub>50</sub> <sup>a</sup> (μM)
1		1.42	12		0.85
2		9.15	13		1.23
3		0.30	14		1.01
4		3.17	15		4.31
5		4.18	16		1.56
6		1.44	17		1.50
7		5.34	18		0.058
8		2.06	19		0.036
9		0.701	20		0.0097
10		0.215			
11		1.93			

<sup>a</sup>Data reported as the mean where  $n \geq 3$ , standard deviations reported in the Supporting Information

synthesis of compounds where the starting piperazines were not commercially available.

The initial route for these compounds centered around the elaboration of amino acids, as it was thought that the chiral

center could be easily purchased and installed. The three-step sequence to form the piperazines proceeded in good yield; however, the base promoted cyclization step was later determined to cause racemization at the chiral center.<sup>29</sup>



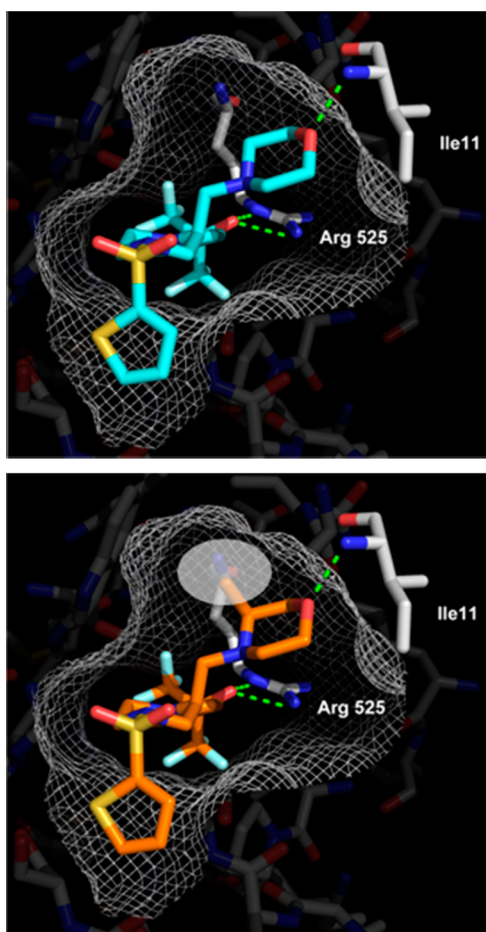


**Figure 4.** Models of compounds **19** (blue) and **20** (orange) bound to hGKRP. The targeted subpocket is highlighted by a gray oval.

Although suitable for synthesis of initial, small (<1 g) deliveries of compound, this issue prompted further investigation of the route as the compounds progressed.<sup>30</sup>

Scheme 3 shows the route for the *N*-linked morpholines. Using commercially available (*R*)-1,4-bis(*tert*-butoxycarbonyl)-piperazine-2-carboxylic acid, the desired morpholine was installed via an amide coupling and subsequent reduction of the amide. After deprotection, the resultant elaborated piperazine was sulfonylated and coupled to the desired aryl bromide to give the final compound. These three synthetic approaches allowed for an extensive array of substitution to be explored at the 2-position of the piperazine ring in an expedient manner.

Zucker diabetic fatty (ZDF) rats were chosen as the disease model for in vivo studies as these rats exhibit a diabetic phenotype as a result of a defect in the glucose-induced translocation of GK from the nucleus.<sup>31</sup> Oral administration of **25** showed a dose-dependent effect on GK translocation in ZDF rats (Figure 6). Immunohistochemistry (IHC) staining was used to monitor the translocation of GK from the cell nucleus. A GK IHC score of 0 represented no detectable nuclear GK, while a score of 4 indicated no GK translocation. As shown in Figure 6, a single dose of 100 mg/kg was sufficient to displace GK from the nucleus at 1 h postdose.<sup>32</sup> In addition, the effect was more robust than with the glucose/fructose positive control.<sup>33</sup>

In the ZDF rat model, compound **25** also displayed robust glucose lowering effects in accordance with the observed GK

**Table 3.** Comparison of Calculated Log Ps

Cmpd	Structure	cLogP <sup>a</sup>
<b>18</b>		4.37
<b>21</b>		3.81
<b>20</b>		4.07
<b>22</b>		3.50

<sup>a</sup>cLogP values were calculated using the PCModels software, version 4.9.2, from Daylight, which is developed and supported by BioByte, Inc., Claremont, CA.

translocation.<sup>22</sup> A 100 mg/kg dose was as efficacious as the standard of care (Metformin) and a known GKA.<sup>34</sup> Moreover, when this same dose was administered to normal Wistar rats, no glucose lowering effect was observed while the GKA caused hypoglycemia. This supported the theory that the GK-GKRP disruptor should carry a lower risk of hypoglycemia. Plasma insulin levels and triglycerides were also found to be unchanged in the ZDF rats after treatment with **25**.

## CONCLUSION

At the onset of this program, it was unclear as to whether the GK-GKRP protein–protein interaction was a tractable small molecule target. A HTS screen identified a compound (**1**) that bound to hGKRP and caused dissociation of the GK-GKRP complex. The X-ray crystal structure revealed that **1** occupied a novel binding pocket on GKRP that was distinct from the sugar binding pocket. Optimization of that initial hit through structure-based design resulted in the identification of compound **25**. This compound had dramatically improved cellular activity while not activating GK directly.<sup>35</sup> Administration of **25** to ZDF rats resulted in robust lowering of blood glucose.<sup>22</sup> The discovery of a novel small molecule binding pocket on GKRP led to the opportunity to modulate the glucose phosphorylation pathway without altering GK kinetics, potentially mitigating the threat of hypoglycemia seen with GKAs. In the following report, we describe the further optimization of **25** to a more drug-like compound with improved potency and exposure.<sup>36</sup>

Table 4. Effect of the Me/CF<sub>3</sub> Moiety

Cmpd	Structure	AlphaScreen IC <sub>50</sub> <sup>a</sup> (μM)	rGK Translocation EC <sub>50</sub> <sup>a</sup> (μM)
23		0.095	0.89
24		0.10	4.76
25 (AMG-1694)		0.021	0.082
26		0.012	0.22

<sup>a</sup>Data reported as the mean where  $n \geq 3$ , standard deviations reported in the Supporting Information.

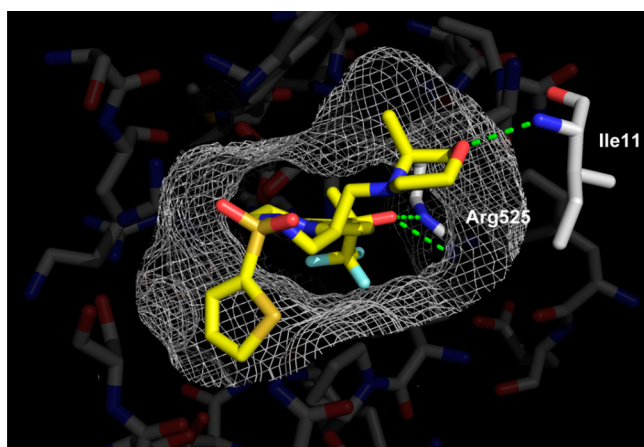


**Figure 5.** The hGKRP X-ray co-crystal structure of **25**. The key hydrogen bonding interactions are shown with green dashed lines, and the surface of the binding site is represented by gray mesh.

## EXPERIMENTAL SECTION

**A. Biology.** 1. *hGK-hGKRP AlphaScreen.* hGKRP–biotin was incubated with compound for 20 min prior to addition of fluorescein–hGK and AlphaScreen beads (PerkinElmer), followed by an additional 2–4 h incubation. hGK–hGKRP binding was detected with a 1:1000

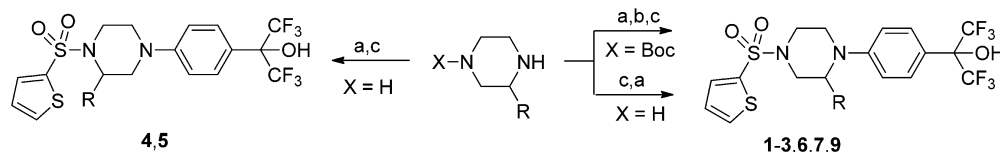
dilution of Alphascreen fluorescein-detection beads (PerkinElmer) at 5 nM GGRP–biotin, 1 nM fluorescein–GK, 1 μM S6P, 20 mM Tris pH 7.5, 0.05% BSA, and 1 mM DTT using an EnVision Instrument (PerkinElmer).

2. *GK Translocation in Rat Hepatocytes.* Rat hepatocytes<sup>37</sup> in maintenance media (Williams E, 10% FBS, 1 × PSG, 1 μg/mL insulin, 100 nM dexamethasone) were plated into a 96-well plate (50000 cells/well) and incubated overnight. Cells were washed twice (200 μL of DMEM no glucose/0.2% BSA) then 100 μL of DMEM (no glucose)/0.2% BSA was added and cells were incubated for 3–4 h at 37 °C. Cells were again washed with DMEM (no glucose) only and test compounds diluted in DMEM (no glucose) were added and incubated for 20 min at 37 °C, followed by addition of 10 μL 25 mM glucose and further incubated for an additional 40 min at 37 °C. Cells were then fixed (100 μL of 8% formaldehyde/PBS), and the plates were incubated at rt for 15 min, washed twice with 200 μL of PBS, then permeabilized (75 μL of 0.3% Triton X-100/PBS) for 10 min. Following two washes with 200 μL of PBS, 50 μL of blocking solution (Li-Cor) was added and incubated for 1 h at rt. Cells were washed (100 μL of 1% goat serum/0.1% Tween in PBS), incubated with 50 μL of anti-GK antibody diluted 1:125 in 1:1 Li-Cor blocking-wash buffer, incubated at 4 °C overnight and, after washing, 50 μL of goat antirabbit AlexaFluor 555 diluted 1:100 and 1 μg/mL of Hoechst 33342 in wash buffer was added to each well and incubated for 1 h at rt. Following washing, 200 μL of PBS was added to each well and imaging was performed using an Operetta system (PerkinElmer).

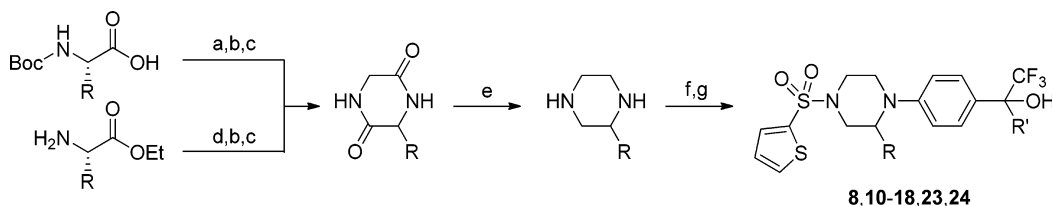
**Table 5.** Activity and PK Properties of Tool Compound **25** in Sprague–Dawley Rat

compd	rGK translocation EC <sub>50</sub> <sup>a</sup> (μM)	RLM CL <sub>int</sub> <sup>b</sup> (μL/min/mg)	CL <sup>c</sup> (L/h/kg)	V <sub>ss</sub> <sup>c</sup> (L/kg)	C <sub>max</sub> <sup>d</sup> (μM)	F <sup>d</sup> (%)	f <sub>u</sub> <sup>e</sup> (%)	C <sub>max</sub> unbound (μM)
25	0.082 ± 0.073	608	4.1	8.25	0.11	7.86	3.7	0.004

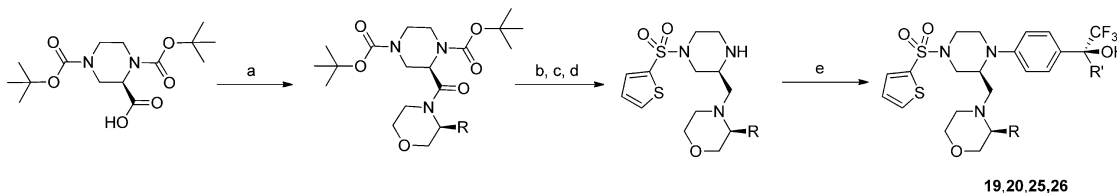
<sup>a</sup>Data reported as the mean ± SD where  $n \geq 3$ . <sup>b</sup>In vitro microsomal stability measurements were conducted in the presence of NADPH at 37 °C for 30 min at a final compound concentration of 1 μM. <sup>c</sup>2 mg/kg intravenous dose (100% DMSO). <sup>d</sup>10 mg/kg oral dose (1% Tween 80, 2% HPMC, 97% water, pH = 7.0). <sup>e</sup>Fraction unbound, determined via rapid equilibrium dialysis.

Scheme 1. Synthesis of Analogues from Commercially Available Substituted Piperazines<sup>a</sup>

<sup>a</sup>Reagents and conditions: (a) 2-(4-bromophenyl)-1,1,1,3,3,3-hexafluoro-2-propanol, RuPhos first-generation precatalyst or Pd<sub>2</sub>dba<sub>3</sub>, RuPhos, NaOtBu, dioxane or toluene, 100 °C; (b) HCl, dioxane; (c) 2-thiophenesulfonyl chloride, NEt<sub>3</sub>, CH<sub>2</sub>Cl<sub>2</sub>.

Scheme 2. Synthesis of Analogues from Amino Acids<sup>a</sup>

<sup>a</sup>Reagents and conditions: (a) glycine methyl ester hydrochloride, HATU, Hünig's base, DMF; (b) TFA, CH<sub>2</sub>Cl<sub>2</sub>; (c) NEt<sub>3</sub> or Hünig's base, MeOH, 70 °C; (d) 2-(*tert*-butoxycarbonylamino)acetic acid HATU, Hünig's base, DMF; (e) BH<sub>3</sub>–DMS or LiAlH<sub>4</sub>, THF, 70 °C; (f) 2-thiophenesulfonyl chloride, NEt<sub>3</sub>, CH<sub>2</sub>Cl<sub>2</sub>; (g) 2-(4-bromophenyl)-1,1,1,3,3,3-hexafluoro-2-propanol or (*R*)-2-(4-bromophenyl)-1,1,1-trifluoro-2-propanol or (*S*)-2-(4-bromophenyl)-1,1,1-trifluoro-2-propanol, RuPhos first-generation precatalyst or Pd<sub>2</sub>dba<sub>3</sub>, RuPhos, NaOtBu, dioxane or toluene, 100 °C.

Scheme 3. Synthesis of *N*-Linked 2-Substituted Piperazine Containing Compounds<sup>a</sup>

<sup>a</sup>Reagents and conditions: (a) HATU, morpholine, Hünig's base, ether; (b) BH<sub>3</sub>–THF, THF; (c) HCl, EtOAc; (d) 2-thiophenesulfonyl chloride, NEt<sub>3</sub>, CH<sub>2</sub>Cl<sub>2</sub>; (e) 2-(4-bromophenyl)-1,1,1,3,3,3-hexafluoro-2-propanol or (*R*)-2-(4-bromophenyl)-1,1,1-trifluoro-2-propanol or (*S*)-2-(4-bromophenyl)-1,1,1-trifluoro-2-propanol, RuPhos first-generation precatalyst or Pd<sub>2</sub>dba<sub>3</sub>, RuPhos, NaOtBu, dioxane or toluene, 100 °C.

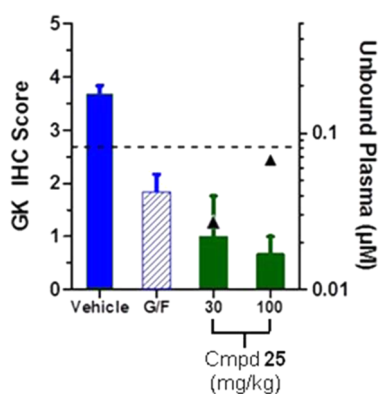


**Figure 6.** In vivo GK translocation (colored bars, left y-axis) and unbound plasma concentrations (black triangles, right y-axis) in ZDF rats following oral administration of **25** (30, 100 mg/kg, 1 h postdose). G/F = glucose:fructose (2 g/kg:0.25 g/kg). The dotted line represents the GK translocation EC<sub>50</sub> (0.080 μM) in rat primary hepatocytes.

**3. In Vivo Studies.** All animals were cared for in accordance to the US National Research Council Guide for the Care and Use of Laboratory Animals, Eighth Edition. Animals were housed two rats per cage at an AAALAC-International-accredited facility in a ventilated microisolator on corn cob bedding. All research protocols were

approved by the Amgen Institutional Animal Care and Use Committee.

**B. Chemistry.** Unless otherwise noted, all reagents were commercially available and used as received. All final compounds possessed purity ≥95% as determined by high performance liquid chromatography (HPLC). The HPLC methods used the following conditions: Zorbax SB-C18 column (50 mm × 3.0 mm, 3.5 μm) at 40 °C with a 1.5 mL/min flow rate; solvent A of 0.1% TFA in water, solvent B of 0.1% TFA in MeCN; 0.0–3.0 min, 5–95% B; 3.0–3.5 min, 95% B; 3.5–3.51 min, 5% B. Flow from the UV detector was split (50:50) to the MS detector which was configured with APIES as an ionizable source. <sup>1</sup>H NMR spectra were recorded on a 400 MHz Bruker NMR spectrometer at ambient temperature. Data are reported as follows: chemical shift (ppm, δ units) from an internal standard, multiplicity (s = singlet, d = doublet, t = triplet, q = quartet, m = multiplet, and br = broad), coupling constant (Hz), and integration. All microwave-assisted reactions were performed in sealed reaction vials using a Personal Chemistry Emrys Optimizer microwave synthesizer. Analytical thin-layer chromatography (TLC) was performed using JT Baker silica gel plates precoated with a fluorescent indicator. Silica gel chromatography was performed using either an ISCO Companion or Biotage medium pressure liquid chromatography system.

**1,1,1,3,3,3-Hexafluoro-2-(4-(4-(2-thiophenylsulfonyl)-1-piperazinyl)phenyl)-2-propanol (1).** A 1 L pressure vessel was charged with 2-(4-bromophenyl)-1,1,1,3,3,3-hexafluoropropan-2-ol (70.8 g, 219 mmol),<sup>38</sup> *tert*-butyl piperazine-1-carboxylate (40.0 g, 215 mmol), 200 mL of toluene, and sodium *tert*-butoxide (43.3 g, 451 mmol). Nitrogen gas was bubbled through the solution for 5 min then chloro(2-dicyclohexylphosphino-2',6'-di-*iso*-propoxy-1,1'-biphenyl)[2-



(2-aminoethylphenyl)]palladium(II), methyl-*tert*-butylether adduct (RuPhos first generation precatalyst) (1.57 g, 2.15 mmol), and 2-dicyclohexyl(2',6'-diisopropoxybiphenyl-2-yl)phosphine (RuPhos) (2.00 g, 4.30 mmol) were added. The vessel was sealed and heated at 65 °C for 2 h. The mixture was diluted with water and extracted with EtOAc. The combined organic extracts were dried (MgSO<sub>4</sub>), filtered, and concentrated to give an oil. To this material was added 200 mL of EtOAc and 200 mL of 4N HCl in dioxane. The solution was heated at 80 °C for 12 h, and the resulting suspension was allowed to cool to rt. The solid precipitate was collected by filtration to give 1,1,1,3,3,3-hexafluoro-2-(4-(1-piperazinyl)phenyl)-2-propanol dihydrochloride (76.2 g, 88%) as a hygroscopic white solid. Generally, the free base or the dihydrochloride salt could be used in the sulfonamide formation. The free base was obtained by neutralizing a solution of the dihydrochloride (in CH<sub>2</sub>Cl<sub>2</sub>) with excess amounts of saturated aqueous NaHCO<sub>3</sub>. <sup>1</sup>H NMR (400 MHz, CD<sub>3</sub>OD) δ = 7.63 (d, *J* = 8.8 Hz, 2 H), 7.11 (d, *J* = 9.0 Hz, 2 H), 3.54–3.48 (m, 4 H), 3.43–3.36 (m, 4 H).

A 100 mL round-bottomed flask was charged with 1,1,1,3,3,3-hexafluoro-2-(4-(1-piperazinyl)phenyl)-2-propanol (2.27 g, 6.92 mmol), 20 mL of CH<sub>2</sub>Cl<sub>2</sub>, and triethylamine (1.45 mL, 10.4 mmol). To this was added 2-thiophenesulfonyl chloride (1.39 mL, 7.61 mmol), and the mixture was stirred at room temperature for 2 h. After that time, the mixture was diluted with water (50 mL) and extracted with EtOAc (100 mL). The combined extracts were dried (MgSO<sub>4</sub>) and concentrated. This oil was purified by column chromatography (120 g silica gel, 0–50% ethyl acetate in hexanes) to give 1,1,1,3,3,3-hexafluoro-2-(4-(4-(thiophen-2-ylsulfonyl)piperazin-1-yl)phenyl)propan-2-ol (2.35 g, 72% yield) as a white solid. <sup>1</sup>H NMR (400 MHz, CDCl<sub>3</sub>) δ 7.70–7.65 (m, 1 H) 7.64–7.56 (m, 3 H), 7.23–7.18 (m, 1 H), 7.02–6.94 (m, 2 H), 3.43–3.36 (m, 4H), 3.33–3.25 (m, 4 H). *m/z* (ESI, +ve ion) 475.0 (M + H)<sup>+</sup>.

**1,1,1,3,3,3-Hexafluoro-2-(4-((2*R*)-2-methyl-4-(2-thiophenylsulfonyl)-1-piperazinyl)phenyl)-2-propanol (2).** Following the procedure reported for compound 3 using *tert*-butyl (3*R*)-3-methyl-1-piperazinecarboxylate delivered 1,1,1,3,3,3-hexafluoro-2-(4-((2*R*)-2-methyl-4-(2-thiophenylsulfonyl)-1-piperazinyl)phenyl)-2-propanol (0.125 g, 49% yield) as a light-yellow solid after column chromatography (0–40% ethyl acetate in hexanes). <sup>1</sup>H NMR (400 MHz, CD<sub>3</sub>OD) δ = 7.87 (d, *J* = 5.1 Hz, 1 H), 7.63 (d, *J* = 3.7 Hz, 1 H), 7.55 (d, *J* = 8.6 Hz, 2 H), 7.25 (t, *J* = 4.4 Hz, 1 H), 6.97 (d, *J* = 9.0 Hz, 2 H), 4.24–4.13 (m, 1 H), 3.76–3.66 (m, 1 H), 3.55–3.44 (m, 2 H), 3.28–3.18 (m, 1 H), 2.86–2.70 (m, 1 H), 2.69–2.53 (m, 1 H), 1.15 (d, *J* = 6.5 Hz, 3 H). *m/z* (ESI, +ve ion) 489.0 (M + H)<sup>+</sup>.

**1,1,1,3,3,3-Hexafluoro-2-(4-((2*S*)-2-methyl-4-(2-thiophenylsulfonyl)-1-piperazinyl)phenyl)-2-propanol (3).** A 20 mL vial was charged with 2-(4-bromophenyl)-1,1,1,3,3,3-hexafluoro-2-propanol (0.725 g, 2.24 mmol), (S)-*tert*-butyl 3-methylpiperazine-1-carboxylate (0.517 g, 2.58 mmol), sodium *tert*-butoxide (0.475 g, 4.94 mmol), and 4 mL of anhydrous toluene. To this was added dicyclohexyl(2',6'-diisopropoxybiphenyl-2-yl)phosphine (RuPhos) (0.016 g, 0.034 mmol) and tris(dibenzylideneacetone)dipalladium (0) (0.010 g, 0.011 mmol). The vial was sealed, and the mixture was heated at 100 °C for 12 h. After that time, the reaction was diluted with water (5 mL) and extracted with EtOAc (2 × 20 mL). The organics were separated and dried (MgSO<sub>4</sub>) to give (3*S*)-3-methyl-4-(4-(2,2,2-trifluoro-1-hydroxy-1-(trifluoromethyl)ethyl)phenyl)-1-piperazinecarboxylate (0.300 g, 30% yield) as an orange oil which was used without purification.

A 100 mL round-bottomed flask was charged with (3*S*)-3-methyl-4-(4-(2,2,2-trifluoro-1-hydroxy-1-(trifluoromethyl)ethyl)phenyl)-1-piperazinecarboxylate (0.250 g, 0.565 mmol) and 10 mL of 4N HCl in dioxane. After 2 h at room temperature, the mixture was concentrated to give (S)-1,1,1,3,3,3-hexafluoro-2-(4-(2-methylpiperazin-1-yl)phenyl)propan-2-ol hydrochloride as a yellow foam (0.214 g, 100% yield) which was used without purification.

A 100 mL round-bottomed flask was charged with (S)-1,1,1,3,3,3-hexafluoro-2-(4-(2-methylpiperazin-1-yl)phenyl)propan-2-ol hydrochloride (0.245 g, 0.647 mmol) and 10 mL of CH<sub>2</sub>Cl<sub>2</sub>. To this was added 2-thiophenesulfonyl chloride (0.142 g, 0.776 mmol) and triethylamine (0.225 mL, 1.617 mmol). After 30 min, the mixture was

concentrated and delivered 1,1,1,3,3,3-hexafluoro-2-(4-((2*S*)-2-methyl-4-(2-thiophenylsulfonyl)-1-piperazinyl)phenyl)-2-propanol (0.150 g, 48% yield) as a light-yellow solid after column chromatography (0–40% ethyl acetate in hexanes). <sup>1</sup>H NMR (400 MHz, CD<sub>3</sub>OD) δ 7.92 (dd, *J* = 5.0, 1.3 Hz, 1 H), 7.66 (dd, *J* = 3.8, 1.3 Hz, 1 H), 7.58 (d, *J* = 8.8 Hz, 2 H), 7.28 (dd, *J* = 5.0, 3.8 Hz, 1 H), 7.00 (d, *J* = 9.2 Hz, 2H), 4.26–4.17 (m, 1H), 3.77–3.71 (m, 1H), 3.57–3.47 (m, 2 H), 3.26 (td, *J* = 11.8, 3.5 Hz, 1 H), 2.80 (dd, *J* = 11.3, 3.3 Hz, 1 H), 2.64 (td, *J* = 11.2, 3.5 Hz, 1 H), 1.18 (*J* = 6.5 Hz, 3 H). *m/z* (ESI, +ve ion) 489.0 (M + H)<sup>+</sup>.

**1,1,1,3,3,3-Hexafluoro-2-(4-((3*S*)-3-methyl-4-(2-thiophenylsulfonyl)-1-piperazinyl)phenyl)-2-propanol (4).** A 20 mL vial was charged with (S)-2-methylpiperazine (0.357 g, 3.56 mmol), 2-(4-bromophenyl)-1,1,1,3,3,3-hexafluoropropan-2-ol (1.00 g, 3.10 mmol), sodium *tert*-butoxide (0.625 g, 6.50 mmol), and 6 mL of toluene. To this was added dicyclohexyl(2',6'-diisopropoxybiphenyl-2-yl)phosphine (RuPhos) (0.022 g, 0.046 mmol) and tris(dibenzylideneacetone)dipalladium (0) (0.014 g, 0.015 mmol). The vial was sealed in heated at 100 °C for 12 h. After that time, the mixture was diluted with water (20 mL) and extracted with EtOAc (2 × 50 mL). The combined extracts were dried (MgSO<sub>4</sub>) and concentrated to give 1,1,1,3,3,3-hexafluoro-2-(4-((3*S*)-3-methyl-1-piperazinyl)phenyl)-2-propanol (0.950 g, 90% yield) as an oil which was used without purification.

A 100 mL round-bottomed flask was charged with 1,1,1,3,3,3-hexafluoro-2-(4-((3*S*)-3-methyl-1-piperazinyl)phenyl)-2-propanol (0.950 g, 2.78 mmol), 5 mL of CH<sub>2</sub>Cl<sub>2</sub>, 2-thiophenesulfonyl chloride (0.583 g, 3.19 mmol), and triethylamine (0.580 mL, 4.16 mmol). After 1 h at room temperature, cat. DMAP (0.010 g, 0.082 mmol) was added. After an additional 30 min, the mixture was concentrated and purified via column chromatography (80 g of silica, 0–40% ethyl acetate in hexanes) to give 1,1,1,3,3,3-hexafluoro-2-(4-((3*S*)-3-methyl-4-(2-thiophenylsulfonyl)-1-piperazinyl)phenyl)-2-propanol (0.425 g, 31% yield) as an off-white solid. <sup>1</sup>H NMR (400 MHz, CDCl<sub>3</sub>) δ = 7.63–7.55 (m, 4 H), 7.12 (dd, *J* = 3.7, 4.9 Hz, 1 H), 6.94 (d, *J* = 9.0 Hz, 2 H), 4.30 (m, 1 H), 3.83 (td, *J* = 3.0, 13.1 Hz, 1 H), 3.66–3.57 (m, 1 H), 3.54–3.38 (m, 2 H), 3.31 (s, 1 H), 3.07 (dd, *J* = 3.5, 12.3 Hz, 1 H), 2.95 (dt, *J* = 3.6, 11.6 Hz, 1 H), 1.30 (d, *J* = 6.7 Hz, 3 H). *m/z* (ESI, +ve ion) 488.7 (M + H)<sup>+</sup>.

**1,1,1,3,3,3-Hexafluoro-2-(4-((3*R*)-3-methyl-4-(2-thiophenylsulfonyl)-1-piperazinyl)phenyl)-2-propanol (5).** Following the procedure reported for compound 4, (R)-2-methylpiperazine delivered 1,1,1,3,3,3-hexafluoro-2-(4-((3*R*)-3-methyl-4-(2-thiophenylsulfonyl)-1-piperazinyl)phenyl)-2-propanol (0.350 g, 38% yield over two steps). <sup>1</sup>H NMR (400 MHz, CDCl<sub>3</sub>) δ = 7.65–7.54 (m, 4 H), 7.12 (dd, *J* = 3.7, 4.9 Hz, 1 H), 6.94 (d, *J* = 9.0 Hz, 2 H), 4.30 (m, 1 H), 3.83 (td, *J* = 3.0, 13.1 Hz, 1 H), 3.68–3.36 (m, 3 H), 3.31 (s, 1 H), 3.07 (dd, *J* = 3.7, 12.3 Hz, 1 H), 2.95 (dt, *J* = 3.6, 11.6 Hz, 1 H), 1.30 (d, *J* = 6.7 Hz, 3 H). *m/z* (ESI, +ve ion) 488.7 (M + H)<sup>+</sup>.

**2-(4-((2*S*)-2-Ethyl-4-(2-thiophenylsulfonyl)-1-piperazinyl)phenyl)-1,1,1,3,3,3-hexafluoro-2-propanol (6).** 2-(4-Bromophenyl)-1,1,1,3,3,3-hexafluoro-2-propanol (0.500 g, 1.55 mmol),<sup>38</sup> *tert*-butyl (3*S*)-3-ethyl-1-piperazinecarboxylate hydrochloride (0.398 g, 1.86 mmol), sodium *tert*-butoxide (0.357 g, 3.71 mmol), dicyclohexyl(2',6'-diisopropoxybiphenyl-2-yl)phosphine (RuPhos) (0.108 g, 0.232 mmol), tris(dibenzylideneacetone)dipalladium (0) (0.080 g, 0.077 mmol), and toluene (3 mL) were added to a high-pressure reaction vessel. This mixture was sealed and heated at 100 °C for 29 h. After that time, the reaction mixture was allowed to cool to room temperature and then partitioned between ethyl acetate (25 mL) and saturated aqueous sodium bicarbonate (10 mL). The layers were separated, the organic material was washed sequentially with saturated aqueous sodium bicarbonate (15 mL) and brine (10 mL), dried (Na<sub>2</sub>SO<sub>4</sub>), filtered, and concentrated to give *tert*-butyl (3*S*)-3-ethyl-4-(4-(2,2,2-trifluoro-1-hydroxy-1-(trifluoromethyl)ethyl)phenyl)-1-piperazinecarboxylate (0.710 g, 100% yield) as a brown solid. The material was used in the next step without purification.

Hydrogen chloride (3.89 mL, 4 M solution in 1,4-dioxane, 15.6 mmol) was added to a stirring solution of *tert*-butyl (3*S*)-3-ethyl-4-(4-(2,2,2-trifluoro-1-hydroxy-1-(trifluoromethyl)ethyl)phenyl)-1-piperazinecarboxylate (0.710 g, 1.56 mmol) and CH<sub>2</sub>Cl<sub>2</sub> (7.8 mL) at room



temperature. After 18 h, the reaction mixture was concentrated to give 2-(4-((2S)-2-ethyl-1-piperazinyl)phenyl)-1,1,1,3,3,3-hexafluoro-2-propanol hydrochloride (0.550 g, 94% yield) as a brown solid. The material was used in the next step without purification.

2-Thiophenesulfonyl chloride (0.282 g, 1.54 mmol) was added to a stirring solution of 2-(4-((2S)-2-ethyl-1-piperazinyl)phenyl)-1,1,1,3,3,3-hexafluoro-2-propanol hydrochloride (0.550 g, 1.54 mmol), *N,N*-diisopropylethylamine (0.807 mL, 4.63 mmol), and DMF (7 mL) at room temperature. After 19 h, the reaction mixture was partitioned between ethyl acetate (20 mL) and saturated aqueous sodium bicarbonate (10 mL). The layers were separated, and the organic material was washed sequentially with saturated aqueous sodium bicarbonate and brine, dried ( $\text{Na}_2\text{SO}_4$ ), and filtered. Silica gel (2.0 g) was added to the filtrate, and the volatiles were removed in vacuo. The residue was subjected to flash chromatography on silica gel (40 g of silica, 20–33% ethyl acetate in hexanes) to give 2-(4-((2S)-2-ethyl-4-(2-thiophenylsulfonyl)-1-piperazinyl)phenyl)-1,1,1,3,3,3-hexafluoro-2-propanol (0.130 g, 17% yield) as an off-white solid.  $^1\text{H}$  NMR (400 MHz,  $\text{CDCl}_3$ ):  $\delta$  7.63 (d,  $J$  = 5.1 Hz, 1 H), 7.59–7.49 (m, 3 H), 7.19–7.13 (m, 1 H), 6.83 (d,  $J$  = 8.0 Hz, 2 H), 3.77 (d,  $J$  = 11.0 Hz, 3 H), 3.49 (d,  $J$  = 12.7 Hz, 1 H), 3.32 (dt,  $J$  = 3.1, 11.9 Hz, 1 H), 3.24 (s, 1 H), 2.74–2.51 (m, 2 H), 1.89 (ddd,  $J$  = 7.3, 9.3, 14.0 Hz, 1 H), 1.60–1.47 (m, 1 H), 0.94 (t,  $J$  = 7.4 Hz, 3 H);  $m/z$  (ESI, +ve ion) 503.0 ( $M + \text{H}$ ) $^+$ .

1,1,1,3,3,3-Hexafluoro-2-(4-((2S)-2-(1-methylethyl)-4-(2-thiophenylsulfonyl)-1-piperazinyl)phenyl)-2-propanol (7). To a solution of (S)-2-isopropylpiperazine dihydrochloride (0.500 g, 2.49 mmol) and triethylamine (1.73 mL, 12.4 mmol) in  $\text{CH}_2\text{Cl}_2$  (10 mL) at rt was added 2-thiophenesulfonyl chloride (0.454 g, 2.49 mmol). After 20 min, the reaction was quenched with aq  $\text{NaHCO}_3$  and  $\text{CH}_2\text{Cl}_2$ , and the organic layer was separated, dried over  $\text{Na}_2\text{SO}_4$ , filtered, and concentrated. The residue was subjected to flash chromatography on silica gel (0–10% MeOH in  $\text{CH}_2\text{Cl}_2$ ) to give (3S)-3-(1-methylethyl)-1-(2-thiophenylsulfonyl)piperazine (0.400 g, 59% yield).  $m/z$  (ESI, +ve ion) 275.0 ( $M + \text{H}$ ) $^+$ .

A solution of (3S)-3-(1-methylethyl)-1-(2-thiophenylsulfonyl)piperazine (400 mg, 1.46 mmol), 2-(4-bromophenyl)-1,1,1,3,3,3-hexafluoropropan-2-ol (565 mg, 1.75 mmol), chloro(2-dicyclohexylphosphino-2',6'-di-*iso*-propoxy-1,1'-biphenyl)[2-(2-aminoethylphenyl)]palladium(II), methyl-*tert*-butylether adduct (RuPhos first generation precatalyst) (59.5 mg, 0.073 mmol), dicyclohexyl(2',6'-diisopropoxybiphenyl-2-yl)phosphine (RuPhos) (68.0 mg, 0.146 mmol), and sodium *t*-butoxide (0.535 mL, 4.37 mmol) in dioxane (10 mL) was stirred at 100 °C overnight. The reaction was concentrated onto silica and purified by flash chromatography on silica gel (0–100% ethyl acetate in hexanes) followed by reverse-phase preparative HPLC using a Phenomenex Gemini  $\text{C}_{18}$  column (30 mm  $\times$  150 mm, 10  $\mu\text{m}$ ) eluting with 0.1% TFA in MeCN/ $\text{H}_2\text{O}$  (10% to 100% over 15 min) to afford 1,1,1,3,3,3-hexafluoro-2-(4-((2S)-2-(1-methylethyl)-4-(2-thiophenylsulfonyl)-1-piperazinyl)phenyl)-2-propanol (5.00 mg, 1% yield).  $^1\text{H}$  NMR (400 MHz,  $\text{CD}_3\text{OD}$ )  $\delta$  7.82 (dd,  $J$  = 1.3, 5.0 Hz, 1 H), 7.59 (dd,  $J$  = 1.3, 3.8 Hz, 1 H), 7.46 (d,  $J$  = 8.8 Hz, 2 H), 7.21 (dd,  $J$  = 3.8, 5.0 Hz, 1 H), 6.87 (d,  $J$  = 9.2 Hz, 2 H), 3.85–3.79 (m, 1 H), 3.78–3.71 (m, 1 H), 3.69–3.57 (m, 2 H), 3.46–3.37 (m, 1 H), 2.56–2.42 (m, 3 H), 1.05 (d,  $J$  = 6.7 Hz, 3 H), 0.84 (d,  $J$  = 6.8 Hz, 3 H).  $m/z$  (ESI, +ve ion) 517.0 ( $M + \text{H}$ ) $^+$ .

1,1,1,3,3,3-Hexafluoro-2-(4-((2S)-2-phenyl-4-(2-thiophenylsulfonyl)-1-piperazinyl)phenyl)-2-propanol (8). Using (2S)-((*tert*-butoxycarbonyl)amino)(phenyl)ethanoic acid and following the procedure for compound 17 gave the desired product 1,1,1,3,3,3-hexafluoro-2-(4-((2S)-2-phenyl-4-(2-thiophenylsulfonyl)-1-piperazinyl)phenyl)-2-propanol (120 mg, 3% yield over six steps) after purification by silica gel chromatography, eluting with 0–70% EtOAc in hexanes.  $^1\text{H}$  NMR (400 MHz,  $\text{CDCl}_3$ )  $\delta$  7.61 (dd,  $J$  = 1.3, 5.0 Hz, 1 H), 7.53 (dd,  $J$  = 1.4, 3.7 Hz, 1 H), 7.46 (d,  $J$  = 8.8 Hz, 2 H), 7.31–7.27 (m, 3 H), 7.25–7.20 (m, 2 H), 7.13 (dd,  $J$  = 3.8, 5.0 Hz, 1 H), 6.89–6.83 (m, 2 H), 4.73–4.67 (m, 1 H), 3.57–3.44 (m, 3 H), 3.43–3.37 (m, 1 H), 3.35–3.29 (m, 2 H).  $m/z$  (ESI, +ve ion) 551.0 ( $M + \text{H}$ ) $^+$ .

2-(4-((2S)-2-Benzyl-4-(2-thiophenylsulfonyl)-1-piperazinyl)phenyl)-1,1,1,3,3,3-hexafluoro-2-propanol (9). Hydrogen chloride (45.2 mL of a 4.0 M solution in 1,4-dioxane, 181 mmol) was added to a stirring solution of *tert*-butyl-(3S)-3-benzyl-1-piperazinecarboxylate (5.00 g, 18.1 mmol) and  $\text{CH}_2\text{Cl}_2$  (36 mL) at room temperature. After 16 h, the reaction mixture was concentrated to give (2S)-2-benzylpiperazine dihydrochloride (4.50 g, 100% yield) as a pale-yellow solid. The material was used in the next step without purification.

2-Thiophenesulfonyl chloride (2.64 g, 14.5 mmol) was added to a stirring solution of (2S)-2-benzylpiperazine hydrochloride (4.50 g, 18.1 mmol), *N,N*-diisopropylethylamine (15.7 mL, 90.0 mmol), and  $\text{CH}_2\text{Cl}_2$  (90 mL) at room temperature. After 3 h, silica gel (29 g) was added to the reaction mixture and the volatiles were removed in vacuo. The residue was subjected to flash chromatography on silica gel (120 g of silica, 2% MeOH in  $\text{CH}_2\text{Cl}_2$ ) to give (3S)-3-benzyl-1-(2-thiophenylsulfonyl)piperazine (5.00 g, 86% yield) as a pale-yellow solid.  $^1\text{H}$  NMR (400 MHz,  $\text{CDCl}_3$ )  $\delta$  7.62 (dd,  $J$  = 1.3, 5.0 Hz, 1 H), 7.54 (dd,  $J$  = 1.4, 3.7 Hz, 1 H), 7.36–7.29 (m, 2 H), 7.27–7.22 (m, 1 H), 7.20–7.13 (m, 3 H), 3.73–3.55 (m, 2 H), 3.13–2.95 (m, 2 H), 2.90–2.72 (m, 2 H), 2.57–2.41 (m, 2 H), 2.23 (t,  $J$  = 10.4 Hz, 1 H).

2-(4-Bromophenyl)-1,1,1,3,3,3-hexafluoro-2-propanol (0.220 g, 0.682 mmol), (3S)-3-benzyl-1-(2-thiophenylsulfonyl)piperazine (0.200 g, 0.620 mmol), sodium *tert*-butoxide (0.185 g, 1.92 mmol), dicyclohexyl(2',6'-diisopropoxybiphenyl-2-yl)phosphine (RuPhos) (0.058 g, 0.124 mmol), tris(dibenzylideneacetone)dipalladium (0) (0.057 g, 0.062 mmol), and toluene (2.5 mL) were added to a high-pressure reaction vessel under a nitrogen atmosphere. The vessel was sealed and was heated at 100 °C for 29 h. After that time, the reaction mixture was allowed to cool to room temperature and then partitioned between ethyl acetate (15 mL) and saturated aqueous sodium bicarbonate (10 mL). The layers were separated, and the organic material was washed sequentially with saturated aqueous sodium bicarbonate (25 mL) and brine (15 mL), dried ( $\text{Na}_2\text{SO}_4$ ), and filtered. The filtrate was concentrated, and the residue was dissolved with  $\text{CH}_2\text{Cl}_2$  (25 mL). Silica gel (3.5 g) was added to the solution, and the volatiles were removed in vacuo. The residue was subjected to flash chromatography on silica gel (25% ethyl acetate in hexanes) to give of 2-(4-((2S)-2-benzyl-4-(2-thiophenylsulfonyl)-1-piperazinyl)phenyl)-1,1,1,3,3,3-hexafluoro-2-propanol (0.048 g, 14% yield) as a colorless solid.  $^1\text{H}$  NMR (400 MHz,  $\text{CDCl}_3$ )  $\delta$  7.72–7.54 (m, 4 H), 7.33–7.14 (m, 6 H), 6.94 (d,  $J$  = 7.2 Hz, 2 H), 4.04 (d,  $J$  = 8.2 Hz, 1 H), 3.91 (d,  $J$  = 9.4 Hz, 1 H), 3.75 (d,  $J$  = 11.2 Hz, 1 H), 3.54 (d,  $J$  = 11.2 Hz, 1 H), 3.42 (t,  $J$  = 10.9 Hz, 1 H), 3.31 (br. s., 1 H), 3.21 (t,  $J$  = 11.7 Hz, 1 H), 2.67–2.48 (m, 3 H).  $m/z$  (ESI, +ve ion) 565.0 ( $M + \text{H}$ ) $^+$ .

2-((4-(2-Thiophenylsulfonyl)-1-(4-(2,2,2-trifluoro-1-hydroxy-1-(trifluoromethyl)ethyl)phenyl)-2-piperazinyl)methyl)phenol (10). Following the procedure for compound 11 using 1-(bromomethyl)-2-methoxybenzene delivered 2-((4-(2-thiophenylsulfonyl)-1-(4-(2,2,2-trifluoro-1-hydroxy-1-(trifluoromethyl)ethyl)phenyl)-2-piperazinyl)-methyl)phenol (21.0 mg, 18% yield over nine steps) as a light-yellow tar.  $^1\text{H}$  NMR (300 MHz,  $\text{CDCl}_3$ )  $\delta$  7.68–7.49 (m, 4 H), 7.24–6.87 (m, 6 H), 6.79–6.68 (m, 1 H), 5.12 (s, 1 H), 4.33–4.19 (m, 1 H), 3.93–3.82 (m, 1 H), 3.71–3.33 (m, 4 H), 3.17 (dd,  $J$  = 13.5, 10.8 Hz, 1 H), 2.86 (dd,  $J$  = 13.5, 3.7 Hz, 1 H), 2.68–2.46 (m, 2 H).  $m/z$  (ESI, +ve ion) 580.7 ( $M + \text{H}$ ) $^+$ .

3-((4-(2-Thiophenylsulfonyl)-1-(4-(2,2,2-trifluoro-1-hydroxy-1-(trifluoromethyl)ethyl)phenyl)-2-piperazinyl)methyl)phenol (11). To a 100 mL round-bottomed flask was added 3-methoxybenzyl bromide (0.730 mL, 5.22 mmol), ethyl *N*-(diphenylmethylene) glycinate (1.40 g, 5.22 mmol), and 5 M sodium hydroxide (5.22 mL, 26.1 mmol) in tetrahydrofuran (20 mL). The reaction mixture was stirred at room temperature for 2 d. After that time, the mixture was diluted with water (30 mL) and extracted with EtOAc (2  $\times$  60 mL). The organic extracts were washed with saturated NaCl (30 mL) and dried over  $\text{Na}_2\text{SO}_4$ . The solution was filtered and concentrated in vacuo to give the crude material as light-yellow oil. The crude product was purified by silica gel chromatography, eluting with 20% EtOAc in hexanes to give ethyl *N*-(diphenylmethylene)-3-methoxyphenylalaninate (1.56 g, 77% yield).  $^1\text{H}$  NMR (300 MHz,  $\text{CDCl}_3$ )  $\delta$  7.66–7.54 (m, 2 H), 7.43–7.28 (m,

6 H), 7.10 (t,  $J = 7.9$  Hz, 1 H), 6.77–6.69 (m, 1 H), 6.69–6.60 (m, 3 H), 6.59–6.54 (m, 1 H), 4.35–4.05 (m, 2 H), 3.65 (s, 3 H), 3.34–3.00 (m, 2 H), 1.36–1.20 (m, 3 H).

To a 100 mL round-bottomed flask was added ethyl *N*-(diphenylmethylenedene)-3-methoxyphenylalaninate (912 mg, 2.35 mmol), 5 M hydrochloric acid (0.471 mL, 2.35 mmol), and tetrahydrofuran (20 mL). The reaction mixture was stirred at room temperature for 1 h. The solvent was removed in vacuo to give the crude product, ethyl 3-methoxyphenylalaninate (526 mg, 100% yield), which was used without further purification.

To a 100 mL round-bottomed flask was added ethyl 3-methoxyphenylalaninate (526 mg, 2.35 mmol), 2-(*tert*-butoxycarbonylamino)acetic acid (454 mg, 2.59 mmol), HATU (1.07 g, 2.82 mmol), Hünig's base (0.819 mL, 4.71 mmol), and DMF (5 mL). The reaction mixture was stirred at room temperature for 2 h then diluted with water (30 mL) and extracted with EtOAc (2 × 50 mL). The organic extract was washed with saturated aqueous NaCl (30 mL) and dried over  $\text{Na}_2\text{SO}_4$ . The solution was filtered and concentrated in vacuo to give the crude material as light-yellow oil. The crude product was purified by silica gel chromatography, eluting with 60% EtOAc in hexanes to give ethyl *N*-(*tert*-butoxycarbonyl)glycyl-3-methoxyphenylalaninate (812 mg, 92% yield).  $^1\text{H}$  NMR (300 MHz,  $\text{CDCl}_3$ )  $\delta = 7.20$  (t,  $J = 7.9$  Hz, 1 H), 6.79 (dd,  $J = 2.3, 8.1$  Hz, 1 H), 6.73–6.62 (m, 2 H), 4.93–4.79 (m, 1 H), 4.26–4.08 (m,  $J = 7.2, 15.6$  Hz, 2 H), 3.91–3.69 (m, 5 H), 3.11 (d,  $J = 5.7$  Hz, 2 H), 1.45 (s, 9 H), 1.33–1.19 (m,  $J = 3.2, 7.2, 7.2$  Hz, 3 H).

To a 100 mL round-bottomed flask was added ethyl *N*-(*tert*-butoxycarbonyl)glycyl-3-methoxyphenylalaninate (812 mg, 2.13 mmol) and TFA (4.38 mL, 67.3 mmol) in dichloromethane (5 mL). The reaction mixture was stirred at room temperature for 30 min. The solvent was removed in vacuo to give crude ethyl glycyl-3-methoxyphenylalaninate (598 mg, 100% yield) as a viscous oil, which was used without purification.

To a 100 mL round-bottomed flask was added ethyl glycyl-3-methoxyphenylalaninate (598 mg, 2.13 mmol), Hünig's base (0.371 mL, 2.13 mmol), and MeOH (20 mL). The reaction mixture was stirred at 75 °C for 24 h. The mixture was cooled to room temperature. The solid formed was collected by filtration and washed with MeOH to give 3-(3-methoxybenzyl)-2,5-piperazinedione (423 mg, 85% yield) as a white solid.  $^1\text{H}$  NMR (300 MHz,  $\text{CD}_3\text{OD}$ )  $\delta = 7.28$ –7.16 (m, 1 H), 6.90–6.84 (m, 1 H), 6.83–6.75 (m, 2 H), 4.31–4.16 (m, 1 H), 3.77 (s, 3 H), 3.51–3.42 (m, 1 H), 3.26–3.16 (m, 1 H), 3.02–2.93 (m, 1 H), 2.82–2.69 (m, 1 H).

To a 100 mL round-bottomed flask was added 3-(3-methoxybenzyl)-2,5-piperazinedione (201 mg, 0.858 mmol), 5 mL of THF, and borane-dimethyl sulfide (0.326 mL, 3.43 mmol). The reaction mixture was stirred at 70 °C for 18 h and then diluted with 1N NaOH (12 mL) and extracted with  $\text{CH}_2\text{Cl}_2$  (2 × 50 mL). The organic extracts were washed with saturated aqueous NaCl (5 mL) and dried over  $\text{Na}_2\text{SO}_4$ . The solution was filtered and concentrated in vacuo to give the crude 2-(3-methoxybenzyl)piperazine (152 mg, 86% yield) as a colorless tar.

To a 100 mL round-bottomed flask was added 2-(3-methoxybenzyl)piperazine (128 mg, 0.621 mmol), 5 mL of  $\text{CH}_2\text{Cl}_2$ , triethylamine (0.129 mL, 0.931 mmol), and 2-thiophenesulfonyl chloride (0.113 mL, 0.621 mmol). The reaction mixture was stirred at 0 °C for 1 h and then diluted with aqueous saturated  $\text{NaHCO}_3$  (5 mL) and extracted with EtOAc (2 × 30 mL). The organic extracts were washed with saturated NaCl (10 mL) and dried over  $\text{Na}_2\text{SO}_4$ . The solution was filtered and concentrated in vacuo to give the crude material as a light-yellow oil. The crude product was purified by silica gel chromatography, eluting with 5% MeOH in EtOAc to give 3-(3-methoxybenzyl)-1-(thiophen-2-ylsulfonyl)piperazine as a colorless oil (162 mg, 74% yield).  $^1\text{H}$  NMR (300 MHz,  $\text{CDCl}_3$ )  $\delta = 7.63$  (dd,  $J = 1.2, 5.0$  Hz, 1 H), 7.55 (dd,  $J = 1.2, 3.7$  Hz, 1 H), 7.23 (d,  $J = 7.9$  Hz, 1 H), 7.16 (dd,  $J = 3.8, 5.0$  Hz, 1 H), 6.84–6.72 (m, 3 H), 4.18–4.09 (m, 1 H), 3.81 (s, 3 H), 3.73–3.59 (m, 2 H), 3.10–2.96 (m, 2 H), 2.90–2.73 (m, 2 H), 2.49 (dd,  $J = 3.3, 10.6$  Hz, 2 H).

To a 50 mL round-bottomed flask was added 3-(3-methoxybenzyl)-1-(thiophen-2-ylsulfonyl)piperazine (48.0 mg, 0.136 mmol), tris-(dibenzylideneacetone)dipalladium (0) (6.24 mg, 6.81  $\mu\text{mol}$ ),

dicyclohexyl(2',4',6'-triisopropyl-[1,1'-biphenyl]-2-yl)phosphine (Ru-Phos) (13.0 mg, 0.027 mmol), sodium *tert*-butoxide (32.7 mg, 0.340 mmol), and 2-(4-bromophenyl)-1,1,1,3,3,3-hexafluoro-2-propanol (52.8 mg, 0.163 mmol) in toluene (2 mL). The reaction mixture was stirred at 100 °C for 18 h. The mixture was cooled to room temperature and then diluted with saturated aqueous  $\text{NH}_4\text{Cl}$  (10 mL) and extracted with EtOAc (2 × 30 mL). The organic extract was washed with saturated NaCl (10 mL) and dried over  $\text{Na}_2\text{SO}_4$ . The solution was filtered and concentrated in vacuo to give the crude material as light-yellow oil. The crude product was purified by silica gel chromatography, eluting with 20% EtOAc in hexanes to give 1,1,1,3,3,3-hexafluoro-2-(4-(2-(3-methoxybenzyl)-4-(thiophen-2-ylsulfonyl)piperazin-1-yl)phenyl)2-propanol (41.0 mg, 51% yield) as a colorless tar.  $^1\text{H}$  NMR (300 MHz,  $\text{CDCl}_3$ )  $\delta = 7.65$ –7.58 (m, 3 H), 7.55 (dd,  $J = 1.3, 3.8$  Hz, 1 H), 7.25 (s, 1 H), 7.15 (dd,  $J = 3.8, 5.0$  Hz, 1 H), 6.98–6.91 (m,  $J = 9.2$  Hz, 2 H), 6.88–6.77 (m, 3 H), 4.08–4.00 (m, 1 H), 3.96–3.88 (m, 1 H), 3.85 (s, 3 H), 3.83–3.76 (m, 1 H), 3.59–3.48 (m, 1 H), 3.47–3.36 (m, 2 H), 3.25–3.15 (m, 1 H), 2.69–2.44 (m, 3 H).

To a 50 mL round-bottomed flask was added 1,1,1,3,3,3-hexafluoro-2-(4-(2-(3-methoxybenzyl)-4-(thiophen-2-ylsulfonyl)piperazin-1-yl)phenyl)2-propanol (38.0 mg, 0.064 mmol) and  $\text{BBr}_3$  (0.025 mL, 0.256 mmol) in DCE (3 mL). The reaction mixture was stirred at 80 °C for 2 h and then diluted with saturated  $\text{NaHCO}_3$  (20 mL) and extracted with EtOAc (2 × 30 mL). The organic extracts were washed with saturated aqueous NaCl (10 mL) and dried over  $\text{Na}_2\text{SO}_4$ . The solution was filtered and concentrated in vacuo to give the crude material as a light-yellow glass. The crude product was purified by silica gel chromatography, eluting with 40% EtOAc in hexanes to give 3-((4-(2-thiophenylsulfonyl)-1-(4-(2,2,2-trifluoro-1-hydroxy-1-(trifluoromethyl)ethyl)phenyl)-2-piperazinyl)methyl)phenol (31.0 mg, 83% yield) as a light-yellow tar.  $^1\text{H}$  NMR (300 MHz,  $\text{CDCl}_3$ )  $\delta = 7.68$ –7.51 (m, 4 H), 7.24–7.11 (m, 2 H), 6.92 (d,  $J = 9.21$  Hz, 2 H), 6.84–6.68 (m, 3 H), 5.56 (s, 1H), 4.08–3.71 (m, 3 H), 3.60–3.32 (m, 3 H), 3.20–3.08 (m, 1 H), 2.66–2.41 (m, 3 H).  $m/z$  (ESI, +ve ion) 580.7 ( $M + H$ ) $^+$ .

4-((4-(2-Thiophenylsulfonyl)-1-(4-(2,2,2-trifluoro-1-hydroxy-1-(trifluoromethyl)ethyl)phenyl)-2-piperazinyl)methyl)phenol (12). Following the procedure for compound 11 using 1-(bromomethyl)-4-methoxybenzene gave 4-((4-(2-thiophenylsulfonyl)-1-(4-(2,2,2-trifluoro-1-hydroxy-1-(trifluoromethyl)ethyl)phenyl)-2-piperazinyl)-methyl)phenol (31.0 mg, 19% yield over nine steps) as a colorless tar.  $^1\text{H}$  NMR (300 MHz,  $\text{CDCl}_3$ )  $\delta = 7.66$ –7.51 (m, 4 H), 7.18–7.08 (m, 3 H), 6.91 (d,  $J = 9.2$  Hz, 2 H), 6.79 (d,  $J = 8.5$  Hz, 2 H), 4.86 (s, 1 H), 4.05–3.85 (m, 2 H), 3.80–3.70 (m, 1 H), 3.58–3.32 (m, 3 H), 3.13 (dd,  $J = 13.01, 10.67$  Hz, 1 H), 2.65–2.42 (m, 3 H).  $m/z$  (ESI, +ve ion) 580.8 ( $M + H$ ) $^+$ .

1,1,1,3,3,3-Hexafluoro-2-(4-(2-(2-methylbenzyl)-4-(2-thiophenylsulfonyl)-1-piperazinyl)phenyl)-2-propanol (13). Following the procedure for compound 11 (omitting the last step) starting from 2-methylbenzyl bromide delivered 1,1,1,3,3,3-hexafluoro-2-(4-(2-(2-methylbenzyl)-4-(2-thiophenylsulfonyl)-1-piperazinyl)phenyl)-2-propanol (132 mg, 31% yield over eight steps) as a mixture of enantiomers.  $^1\text{H}$  NMR (300 MHz,  $\text{CDCl}_3$ )  $\delta = 7.68$ –7.47 (m, 4 H), 7.26–7.24 (m, 1 H), 7.14 (d,  $J = 1.3$  Hz, 4 H), 6.94 (d,  $J = 9.1$  Hz, 2 H), 4.08–4.00 (m, 1 H), 3.95–3.86 (m, 1 H), 3.76–3.67 (m, 1 H), 3.59–3.40 (m, 2 H), 3.33–3.20 (m, 1 H), 2.70–2.49 (m, 3 H), 2.20 (s, 3 H).  $m/z$  (ESI, +ve ion) 578.8 ( $M + H$ ) $^+$ .

1,1,1,3,3,3-Hexafluoro-2-((4-(2-(3-methylbenzyl)-4-(2-thiophenylsulfonyl)-1-piperazinyl)phenyl)-2-propanol Hydrochloride (14). A 100 mL round-bottomed flask was charged with (S)-2-(*tert*-butoxycarbonylamino)-3-*m*-tolylpropanoic acid (2.60 g, 9.31 mmol), HATU (4.25 g, 11.17 mmol), glycine methyl ester hydrochloride (1.29 g, 10.2 mmol), and 20 mL of DMF. To this was added Hünig's base (3.34 mL, 18.6 mmol). After 1 h at room temperature, the mixture was diluted with water (100 mL) and extracted with ether (2 × 200 mL). The layers were separated, and the organic extracts were washed with water (2 × 100 mL) and brine (50 mL), dried ( $\text{MgSO}_4$ ), and concentrated to give methyl *N*-(*tert*-butoxycarbonyl)-3-methyl-*L*-phenylalanylglycinate (3.10 g, 95% yield) as a yellow oil that was



used directly in the next step.  $^1\text{H}$  NMR (400 MHz,  $\text{CDCl}_3$ )  $\delta$  = 7.24–7.16 (m, 1 H), 7.03 (s, 3 H), 6.46–6.29 (m, 1 H), 4.98 (br. s, 1 H), 4.41 (br. s, 1 H), 4.13–3.90 (m, 2 H), 3.74 (s, 3 H), 3.12–2.98 (m, 2 H), 2.33 (s, 3 H), 1.42 (s, 9 H).

A 150 mL round-bottomed flask was charged with methyl *N*-(*tert*-butoxycarbonyl)-3-methyl-L-phenylalanyl-glycinate (3.31 g, 8.85 mmol), 10 mL of  $\text{CH}_2\text{Cl}_2$ , and 10 mL of TFA. After 30 min, the mixture was concentrated then redissolved in MeOH (100 mL) and triethylamine (15 mL, 108 mmol) and heated to 70 °C overnight. After that time, the white precipitate that had formed was collected by filtration to give 3-(3-methylbenzyl)-2,5-piperazinedione (1.92 g, 100% yield) as a white solid. Heating for this amount of time with base resulted in racemization of the chiral center.  $^1\text{H}$  NMR (400 MHz,  $\text{CD}_3\text{OD}$ )  $\delta$  = 7.21 (t,  $J$  = 7.4 Hz, 1 H), 7.17–7.12 (m, 1 H), 7.09–6.99 (m, 2 H), 4.23 (t,  $J$  = 4.4 Hz, 1 H), 3.45 (d,  $J$  = 17.8 Hz, 1 H), 3.36–3.32 (m, 1 H), 2.99 (dd,  $J$  = 4.7, 13.7 Hz, 1 H), 2.68 (dd,  $J$  = 0.9, 17.7 Hz, 1 H), 2.33 (s, 3 H).

A 150 mL round-bottomed flask was charged with 3-(3-methylbenzyl)-2,5-piperazinedione (1.93 g, 8.85 mmol), 20 mL of THF, and lithium aluminum hydride (38.5 mL, 1 M in THF, 38.5 mmol). After heating to 70 °C for 1 h, the mixture was cooled to room temperature where sodium sulfate decahydrate (10 g) was slowly added. After stirring at room temperature for 1 h, the mixture was filtered and the filtrate was concentrated to give 2-(3-methylbenzyl)-piperazine (0.700 g, 38% yield).  $^1\text{H}$  NMR (400 MHz,  $\text{CD}_3\text{OD}$ )  $\delta$  = 7.22–7.13 (m, 1 H), 7.08–6.97 (m, 3 H), 2.92–2.81 (m, 4 H), 2.77–2.64 (m, 2 H), 2.59 (d,  $J$  = 6.8 Hz, 2 H), 2.38 (dd,  $J$  = 10.8, 12.9 Hz, 1 H), 2.32 (s, 3 H).

A 100 mL round-bottomed flask was charged with 2-(3-methylbenzyl)piperazine (0.700 g, 3.68 mmol), 15 mL of  $\text{CH}_2\text{Cl}_2$ , triethylamine (0.513 mL, 3.68 mmol), and 2-thiophenylsulfonyl chloride (0.672 g, 3.68 mmol). After 30 min at room temperature, the mixture was diluted with aq  $\text{NaHCO}_3$  (50 mL) and  $\text{CH}_2\text{Cl}_2$  (50 mL). The organics were separated, dried ( $\text{Na}_2\text{SO}_4$ ), and concentrated. The crude product was purified by silica gel chromatography, eluting with 0–10% (2 M  $\text{NH}_3$  in MeOH) in  $\text{CH}_2\text{Cl}_2$  to give 3-(3-methylbenzyl)-1-(2-thiophenylsulfonyl)piperazine (0.350 g, 28% yield).  $^1\text{H}$  NMR (400 MHz,  $\text{CD}_3\text{OD}$ )  $\delta$  = 7.98 (dd,  $J$  = 1.3, 5.0 Hz, 1 H), 7.69 (dd,  $J$  = 1.3, 3.8 Hz, 1 H), 7.33–7.28 (m, 2 H), 7.21–7.17 (m, 1 H), 7.16–7.14 (m, 1 H), 7.12–7.08 (m, 1 H), 3.85–3.77 (m, 1 H), 3.75–3.67 (m, 2 H), 3.56–3.50 (m, 1 H), 3.32–3.21 (m, 2 H), 2.97–2.87 (m, 2 H), 2.76–2.65 (m, 1 H), 2.40 (s, 3 H).

A 10 mL microwave vial was charged with 3-(3-methylbenzyl)-1-(2-thiophenylsulfonyl)piperazine (150 mg, 0.446 mmol), 2-(4-bromophenyl)-1,1,1,3,3,3-hexafluoro-2-propanol (180 mg, 0.557 mmol), sodium *tert*-butoxide (0.150 mg, 1.56 mmol), dicyclohexyl(2',6'-diisopropoxybiphenyl-2-yl)phosphine (RuPhos) (18.7 g, 0.040 mmol), tris(dibenzylideneacetone)dipalladium (0) (12.3 mg, 0.013 mmol), and 2 mL of toluene. The mixture was sealed and heated at 100 °C overnight and then concentrated onto silica and purified by silica gel chromatography, eluting with 0–60% EtOAc in hexanes to give the desired product. The free base was acidified with 4N HCl in dioxane to provide 1,1,1,3,3,3-hexafluoro-2-(4-(2-(3-methylbenzyl)-4-(2-thiophenylsulfonyl)-1-piperazinyl)phenyl)-2-propanol hydrochloride (30 mg, 11% yield) as a mixture of enantiomers.  $^1\text{H}$  NMR (400 MHz,  $\text{CD}_3\text{OD}$ )  $\delta$  = 7.87–7.83 (m, 1 H), 7.62–7.58 (m, 3 H), 7.24–7.21 (m, 1 H), 7.19–7.14 (m, 1 H), 7.08–6.99 (m, 5 H), 4.17–4.11 (m, 1 H), 3.88–3.82 (m, 1 H), 3.68–3.56 (m, 2 H), 3.42–3.34 (m, 1 H), 3.12–3.04 (m, 1 H), 2.62–2.53 (m, 2 H), 2.51–2.46 (m, 1 H), 2.31 (s, 3 H).  $m/z$  (ESI, +ve ion) 578.8 ( $\text{M} + \text{H}$ ) $^+$ .

**1,1,1,3,3,3-Hexafluoro-2-(4-(2-(4-methylbenzyl)-4-(2-thiophenylsulfonyl)-1-piperazinyl)phenyl)-2-propanol hydrochloride (15).** Following the procedure for compound 14 starting from *N*-(*tert*-butoxycarbonyl)-4-methyl-L-phenylalanine delivered 1,1,1,3,3,3-hexafluoro-2-(4-(2-(4-methylbenzyl)-4-(2-thiophenylsulfonyl)-1-piperazinyl)phenyl)-2-propanol hydrochloride (10.0 mg, 1% yield over six steps) as a mixture of enantiomers.  $^1\text{H}$  NMR (400 MHz,  $\text{CD}_3\text{OD}$ )  $\delta$  = 7.86–7.83 (m, 1 H), 7.61–7.56 (m, 3 H), 7.24–7.20 (m, 1 H), 7.13–7.07 (m, 4 H), 7.05–7.00 (m, 2 H), 4.15–4.08 (m, 1 H), 3.86–3.81 (m, 1 H), 3.66–3.55 (m, 2 H), 3.41–3.33 (m, 1 H), 3.10–3.03

(m, 1 H), 2.61–2.53 (m, 2 H), 2.51–2.46 (m, 1 H), 2.29 (s, 3 H).  $m/z$  (ESI, +ve ion) 578.8 ( $\text{M} + \text{H}$ ) $^+$ .

**1,1,1,3,3,3-Hexafluoro-2-(4-(2-(4-pyridinylmethyl)-4-(2-thiophenylsulfonyl)-1-piperazinyl)phenyl)-2-propanol (16).** To a solution of (*S*)-2-((*tert*-butoxycarbonyl)amino)-3-(pyridin-4-yl)propanoic acid (2.50 g, 9.39 mmol), HATU (3.93 g, 10.3 mmol), and glycine methyl ester hydrochloride (1.30 g, 10.3 mmol) in DMF (10 mL) was added Hünig's base (4.90 mL, 28.2 mmol). After 30 min, another 2 equiv of Hünig's base (9.80 mL, 56.4 mmol), 0.5 equiv of HATU (1.97 g, 5.17 mmol), and 0.5 equiv of glycine methyl ester hydrochloride (0.649 g, 5.17 mmol) were added. After stirring overnight, the reaction was complete and was diluted with water and  $\text{Et}_2\text{O}$  and the organic layer separated, washed with  $\text{NaHCO}_3$  and brine, dried ( $\text{Na}_2\text{SO}_4$ ), filtered, and concentrated. The crude residue was dissolved in  $\text{CH}_2\text{Cl}_2$  (10 mL) and TFA (10.46 mL, 141 mmol) and stirred at rt for 1 h. The reaction was concentrated in vacuo and azeotroped with toluene twice to yield (*S*)-methyl 2-(2-((*tert*-butoxycarbonyl)amino)-3-(pyridin-4-yl)propanamido)acetate (2.00 g, 5.93 mmol) as the TFA salt that was used directly in the next reaction. A solution of (*S*)-methyl 2-(2-((*tert*-butoxycarbonyl)amino)-3-(pyridin-4-yl)propanamido)acetate (2.0 g, 5.93 mmol) in MeOH (30 mL) and triethylamine (8.25 mL, 59.3 mmol) was heated at 65 °C for 2 days. A precipitate formed, and this was collected by filtration after cooling of the reaction. The resultant 3-(pyridin-4-ylmethyl)piperazine-2,5-dione (1.10 g, 90% yield over 3 steps) was isolated as a hygroscopic solid that was a mixture of enantiomers.

To a suspension of 3-(pyridin-4-ylmethyl)piperazine-2,5-dione (1.10 g, 5.36 mmol) and sodium borohydride (0.811 g, 21.4 mmol) in THF (10 mL) at rt was added boron trifluoride diethyl etherate (1.32 mL, 10.7 mmol). The reaction was stirred for 2 days before being quenched with MeOH and concentrated in vacuo. The crude solid was slurried with EtOAc and filtered, and the filtrate was acidified with 4N HCl in dioxane. The resultant solid was collected and dried under high vacuum overnight. The impure 2-(pyridin-4-ylmethyl)piperazine trihydrochloride was concentrated onto silica and purified by chromatography, eluting with 0–10% (2 M  $\text{NH}_3$  in MeOH) in  $\text{CH}_2\text{Cl}_2$  to give 2-(pyridin-4-ylmethyl)piperazine (50.0 mg, 3% yield).

To a solution of 2-(pyridin-4-ylmethyl)piperazine (50.0 mg, 0.282 mmol) in  $\text{CH}_2\text{Cl}_2$  (5 mL) and thiophene-2-sulfonyl chloride (51.5 mg, 0.282 mmol) was added triethylamine (0.206 mL, 0.282 mmol). After 5 min, the reaction was quenched with MeOH and concentrated onto silica. Purification by silica gel chromatography, eluting with 0–10% (2 M  $\text{NH}_3$  in MeOH) in  $\text{CH}_2\text{Cl}_2$ , gave the desired material 3-(pyridin-4-ylmethyl)-1-(thiophen-2-ylsulfonyl)piperazine (80.0 mg, 88% yield).

A solution of 3-(pyridin-4-ylmethyl)-1-(thiophen-2-ylsulfonyl)piperazine (80.0 mg, 0.247 mmol), 2-(4-bromophenyl)-1,1,1,3,3,3-hexafluoropropan-2-ol (120 mg, 0.371 mmol), tris(dibenzylideneacetone)dipalladium (0) (45.3 mg, 0.049 mmol), dicyclohexyl(2',6'-diisopropoxy-[1,1'-biphenyl]-2-yl)phosphine (RuPhos) (46.2 mg, 0.099 mmol), sodium *tert*-butoxide (0.091 mL, 0.742 mmol) in toluene (3 mL), and DMF (1 mL) was heated in a sealed tube at 100 °C overnight. The reaction was concentrated onto silica and purified by chromatography, eluting with 0–100% Hex/EtOAc to give 1,1,1,3,3,3-hexafluoro-2-(4-(2-(4-pyridinylmethyl)-4-(2-thiophenylsulfonyl)-1-piperazinyl)phenyl)-2-propanol (4.00 mg, 3% yield).  $^1\text{H}$  NMR (400 MHz,  $\text{CD}_3\text{OD}$ )  $\delta$  = 8.41 (d,  $J$  = 6.1 Hz, 2 H), 7.88–7.84 (m, 1 H), 7.63–7.55 (m, 3 H), 7.33 (d,  $J$  = 5.9 Hz, 2 H), 7.26–7.20 (m, 1 H), 7.03 (d,  $J$  = 9.2 Hz, 2 H), 4.35–4.26 (m, 1 H), 3.87 (d,  $J$  = 10.8 Hz, 1 H), 3.65–3.55 (m, 2 H), 3.47–3.37 (m, 1 H), 3.20 (dd,  $J$  = 10.1, 13.0 Hz, 1 H), 2.76 (dd,  $J$  = 4.0, 13.0 Hz, 1 H), 2.63–2.52 (m, 2 H).  $m/z$  (ESI, +ve ion) 566.0 ( $\text{M} + \text{H}$ ) $^+$ .

**2-(4-((2*S*)-2-(Cyclohexylmethyl)-4-(2-thiophenylsulfonyl)-1-piperazinyl)phenyl)-1,1,1,3,3,3-hexafluoro-2-propanol (17).** A 100 mL round-bottomed flask was charged with *N*-(*tert*-butoxycarbonyl)-3-cyclohexyl-L-alanine (2.00 g, 7.37 mmol), HATU (3.08 g, 8.11 mmol), glycine methyl ester hydrochloride (1.02 g, 8.11 mmol), and 20 mL of DMF. To this was added Hünig's base (2.57 mL, 14.7 mmol). After 5 min at rt, the mixture was diluted with water (100 mL) and extracted with ether (2  $\times$  200 mL). The layers were separated, and the organic extracts were washed with water (2  $\times$  100 mL) and brine

(50 mL), dried ( $\text{MgSO}_4$ ), and concentrated to give methyl *N*-(*tert*-butoxycarbonyl)-3-cyclohexyl-L-alanylglycinate (2.52 g, 100% yield) as a yellow oil that was used directly in the next step.

A 150 mL round-bottomed flask was charged with methyl *N*-(*tert*-butoxycarbonyl)-3-cyclohexyl-L-alanylglycinate (2.52 g, 7.37 mmol), 10 mL of  $\text{CH}_2\text{Cl}_2$ , and 10 mL of TFA. After 30 min, the mixture was concentrated then redissolved in 2 M ammonia in MeOH (20 mL) and stirred at rt overnight. After that time, the white precipitate that had formed was collected by filtration to give (3*S*)-3-(cyclohexylmethyl)-2,5-piperazinedione (1.30 g, 84% yield).

A 150 mL round-bottomed flask was charged with (3*S*)-3-(cyclohexylmethyl)-2,5-piperazinedione (1.10 g, 5.23 mmol), 30 mL of THF, and lithium aluminum hydride (20.9 mL, 1 M in THF, 20.9 mmol). After heating to 70 °C overnight, the mixture was cooled to room temperature where sodium sulfate decahydrate (10 g) was slowly added. After stirring for 1 h, the mixture was filtered, and the filtrate was concentrated to give (2*S*)-2-(cyclohexylmethyl)piperazine (0.954 g, 100% yield) as a colorless oil that was used crude in the next reaction.

A 100 mL round-bottomed flask was charged with (2*S*)-2-(cyclohexylmethyl)piperazine (0.950 g, 5.21 mmol),  $\text{CH}_2\text{Cl}_2$  (30 mL), triethylamine (2.17 mL, 15.6 mmol), and 2-thiophenylsulfonyl chloride (0.952 mL, 5.21 mmol). After 10 min at room temperature, the mixture was diluted with aq  $\text{NaHCO}_3$  (50 mL) and  $\text{CH}_2\text{Cl}_2$  (50 mL), the organics were separated, dried ( $\text{Na}_2\text{SO}_4$ ), and concentrated. The crude product was purified by silica gel chromatography, eluting with 0–10% MeOH in  $\text{CH}_2\text{Cl}_2$  to give (3*S*)-3-(cyclohexylmethyl)-1-(2-thiophenylsulfonyl)piperazine (1.40 g, 82% yield).

A 100 mL round-bottomed flask was charged with (3*S*)-3-(cyclohexylmethyl)-1-(2-thiophenylsulfonyl)piperazine (0.700 g, 2.13 mmol), 2-(4-bromophenyl)-1,1,1,3,3,3-hexafluoro-2-propanol (0.826 g, 2.56 mmol), sodium *tert*-butoxide (0.783 g, 6.39 mmol), dicyclohexyl(2',6'-diisopropoxybiphenyl-2-yl)phosphine (RuPhos) (0.099 g, 0.213 mmol), chloro(2-dicyclohexylphosphino-2',6'-diisopropoxy-1,1'-biphenyl)[2-(2-aminoethylphenyl)]palladium(II), methyl-*tert*-butylether adduct (RuPhos first generation precatalyst) (0.087 g, 0.107 mmol), and 10 mL of dioxane. The mixture was heated at 100 °C overnight and then concentrated onto silica and purified by silica gel chromatography, eluting with 0–100% EtOAc in hexanes to give 2-(4-((2*S*)-2-(cyclohexylmethyl)-4-(2-thiophenylsulfonyl)-1-piperazinyl)phenyl)-1,1,1,3,3,3-hexafluoro-2-propanol (20.0 mg, 2% yield) as a single enantiomer.  $^1\text{H}$  NMR (400 MHz,  $\text{CD}_3\text{OD}$ )  $\delta$  = 7.86 (dd,  $J$  = 1.1, 5.0 Hz, 1 H), 7.63 (dd,  $J$  = 1.2, 3.9 Hz, 1 H), 7.52 (d,  $J$  = 8.8 Hz, 2 H), 7.24 (dd,  $J$  = 3.9, 4.9 Hz, 1 H), 6.92 (d,  $J$  = 9.2 Hz, 2 H), 4.17–4.05 (m, 1 H), 3.79–3.72 (m, 1 H), 3.70–3.61 (m, 1 H), 3.56–3.47 (m, 1 H), 3.28–3.21 (m, 1 H), 2.71–2.62 (m, 1 H), 2.62–2.44 (m, 1 H), 1.83–1.53 (m, 6 H), 1.34–1.10 (m, 5 H), 0.98–0.72 (m, 2 H).  $m/z$  (ESI, +ve ion) 571.1 ( $M + \text{H}$ )<sup>+</sup>.

1,1,1,3,3,3-Hexafluoro-2-(4-((2*S*)-2-(tetrahydro-2*H*-pyran-4-ylmethyl)-4-(2-thiophenylsulfonyl)-1-piperazinyl)phenyl)-2-propanol (**18**). To a solution of tetrahydro-2*H*-pyran-4-carbaldehyde (5.00 g, 43.8 mmol) in  $\text{CH}_2\text{Cl}_2$  (100 mL) at rt was added (±)-Boc- $\alpha$ -phosphonoglycine trimethyl ester (15.0 g, 50.4 mmol) followed by DBU (7.53 mL, 50.4 mmol). The reaction was stirred overnight before being diluted with water (100 mL) and extracted with  $\text{CH}_2\text{Cl}_2$  (2  $\times$  200 mL). The layers were separated, and the organic extracts were washed with water (2  $\times$  100 mL), dried ( $\text{MgSO}_4$ ), and concentrated. The crude material was purified by column chromatography (0–70% hexanes in EtOAc) to give (2*E*)-2-((*tert*-butoxycarbonyl)amino)-3-(tetrahydro-2*H*-pyran-4-yl)-2-propenoate (9.10 g, 73% yield).  $^1\text{H}$  NMR (400 MHz,  $\text{CD}_3\text{OD}$ )  $\delta$  = 6.42–6.23 (m, 1 H), 4.02–3.87 (m, 2 H), 3.75 (s, 3 H), 3.46 (dt,  $J$  = 2.2, 11.6 Hz, 2 H), 2.77–2.60 (m, 1 H), 1.59 (d,  $J$  = 2.0 Hz, 2 H), 1.51 (d,  $J$  = 4.5 Hz, 2 H), 1.46 (s, 9 H).

A 250 mL pressure tube was charged with (2*E*)-2-((*tert*-butoxycarbonyl)amino)-3-(tetrahydro-2*H*-pyran-4-yl)-2-propenoate (8.75 g, 30.7 mmol), MeOH (100 mL), and rhodium [(1*R*,1'*R*,2*R*,2'*R*)-2,2'-bis(1,1-dimethylethyl)-2,2',3,3'-tetrahydro-1,1'-bi-1*H*-isophosphindole- $\kappa$ P2, $\kappa$ P2'][(1,2,5,6- $\eta$ )-1,5-cyclooctadiene] tetrafluoroborate (209 mg, 0.307 mmol). The mixture was stirred under a 50 psig hydrogen atmosphere for 3 h. The mixture was filtered through

a pad of silica, washed with 1:1 EtOAc:hexanes, and concentrated to give methyl *N*-(*tert*-butoxycarbonyl)-3-(tetrahydro-2*H*-pyran-4-yl)-L-alaninate (8.81 g, 100% yield) that was used crude in the next reaction.

A 500 mL round bottomed flask was charged with methyl *N*-(*tert*-butoxycarbonyl)-3-(tetrahydro-2*H*-pyran-4-yl)-L-alaninate (8.81 g, 30.7 mmol), 100 mL of THF, 100 mL of water, and lithium hydroxide (2.20 g, 92.0 mmol). After stirring overnight at room temperature, the mixture was concentrated and acidified to pH 3. The mixture was extracted with EtOAc, dried, and concentrated to give *N*-(*tert*-butoxycarbonyl)-3-(tetrahydro-2*H*-pyran-4-yl)-L-alanine (8.00 g, 95% yield) as a white solid.  $^1\text{H}$  NMR (400 MHz,  $\text{CD}_3\text{OD}$ )  $\delta$  = 4.23–4.14 (m, 1 H), 3.98–3.85 (m, 2 H), 3.45–3.34 (m, 2 H), 1.76–1.55 (m, 5 H), 1.44 (s, 9 H), 1.37–1.22 (m, 2 H).

A 100 mL round-bottomed flask was charged with *N*-(*tert*-butoxycarbonyl)-3-(tetrahydro-2*H*-pyran-4-yl)-L-alanine (8.00 g, 29.3 mmol), HATU (13.4 g, 35.1 mmol), glycine methyl ester hydrochloride (4.04 g, 32.2 mmol), and 30 mL of DMF. To this was added Hünig's base (12.8 mL, 73.2 mmol). After 30 min at room temperature, the mixture was diluted with water (300 mL) and extracted with EtOAc (2  $\times$  400 mL). The layers were separated, and the organic extracts were washed with water (2  $\times$  200 mL) and brine (100 mL), dried ( $\text{MgSO}_4$ ), and concentrated to give methyl *N*-(*tert*-butoxycarbonyl)-3-(tetrahydro-2*H*-pyran-4-yl)-L-alanylglycinate (8.05 g, 80% yield) as a yellow oil.  $^1\text{H}$  NMR (400 MHz,  $\text{CD}_3\text{OD}$ )  $\delta$  = 4.22–4.14 (m, 1 H), 4.05–3.97 (m, 1 H), 3.96–3.84 (m, 3 H), 3.72 (s, 3 H), 3.47–3.34 (m, 2 H), 1.76–1.54 (m, 5 H), 1.45 (s, 9 H), 1.24 (s, 2 H).

A 250 mL round-bottomed flask was charged with methyl *N*-(*tert*-butoxycarbonyl)-3-(tetrahydro-2*H*-pyran-4-yl)-L-alanylglycinate (3.00 g, 8.71 mmol), 10 mL of  $\text{CH}_2\text{Cl}_2$ , and 5 mL of TFA. After 10 min, the mixture was concentrated then redissolved in 2*N*  $\text{NH}_3$  in MeOH (20 mL) and stirred at rt for 4 h. After that time, the reaction was concentrated and triturated with ether to give (3*S*)-3-(tetrahydro-2*H*-pyran-4-ylmethyl)-2,5-piperazinedione (1.44 g, 78% yield) as a white solid.  $^1\text{H}$  NMR (400 MHz,  $\text{DMSO}-d_6$ )  $\delta$  = 3.89–3.77 (m, 3 H), 3.73 (dt,  $J$  = 2.9, 6.7 Hz, 1 H), 3.62 (dd,  $J$  = 3.1, 17.2 Hz, 1 H), 3.30–3.22 (m, 2 H), 3.10 (d,  $J$  = 7.0 Hz, 1 H), 1.78–1.67 (m, 1 H), 1.66–1.52 (m, 4 H), 1.14–1.00 (m, 1 H).

A 250 mL round-bottomed flask was charged with (3*S*)-3-(tetrahydro-2*H*-pyran-4-ylmethyl)-2,5-piperazinedione (1.44 g, 6.78 mmol), 50 mL of THF, and LAH (27.1 mL, 1 M in THF, 27.1 mmol). After refluxing for 2 h, the mixture was cooled to room temperature where sodium sulfate decahydrate (10 g) was added. After stirring at room temperature for 1 h, the mixture was filtered to give (2*S*)-2-(tetrahydro-2*H*-pyran-4-ylmethyl)piperazine (0.950 g, 76% yield) as a colorless oil. The purity of this material was increased by dissolution in EtOAc and the addition of 4*N* HCl in dioxane, the resultant (2*S*)-2-(tetrahydro-2*H*-pyran-4-ylmethyl)piperazine dihydrochloride was collected by filtration.  $^1\text{H}$  NMR (400 MHz,  $\text{CD}_3\text{OD}$ )  $\delta$  = 3.91 (dd,  $J$  = 3.4, 11.2 Hz, 2 H), 3.47–3.36 (m, 2 H), 2.96–2.82 (m, 3 H), 2.81–2.59 (m, 3 H), 2.30 (dd,  $J$  = 10.4, 12.1 Hz, 1 H), 1.72–1.57 (m, 3 H), 1.33–1.15 (m, 4 H).

To a solution of (S)-2-((tetrahydro-2*H*-pyran-4-yl)methyl)-piperazine dihydrochloride (700 mg, 2.72 mmol) in  $\text{CH}_2\text{Cl}_2$  (10 mL) at rt was added triethylamine (1.90 mL, 13.6 mmol) and thiophene-2-sulfonyl chloride (547 mg, 2.99 mmol). After 10 min, the reaction was diluted with water and  $\text{CH}_2\text{Cl}_2$ . The organic layer was separated, dried over  $\text{Na}_2\text{SO}_4$ , filtered, and concentrated to give (3*S*)-3-(tetrahydro-2*H*-pyran-4-ylmethyl)-1-(2-thiophenylsulfonyl)piperazine (900 mg, 100% yield), which was used directly in the next reaction.

A solution of (3*S*)-3-(tetrahydro-2*H*-pyran-4-ylmethyl)-1-(2-thiophenylsulfonyl)piperazine (300 mg, 0.908 mmol), 2-(4-bromophenyl)-1,1,1,3,3,3-hexafluoropropan-2-ol (352 mg, 1.09 mmol), chloro(2-dicyclohexylphosphino-2',6'-diisopropoxy-1,1'-biphenyl)[2-(2-aminoethylphenyl)]palladium(II), methyl-*tert*-butylether adduct (RuPhos first generation precatalyst) (37.1 mg, 0.045 mmol), 2-dicyclohexylphosphino-2',6'-dimethoxy-1,1'-biphenyl (RuPhos) (37.3 mg, 0.091 mmol), and sodium *tert*-butoxide (0.278 mL, 2.27 mmol)



was heated in a sealed tube at 100 °C overnight. The reaction was then diluted with water and extracted with EtOAc, and the organic layer was separated, dried over Na<sub>2</sub>SO<sub>4</sub>, filtered, and concentrated. Purified by silica gel chromatography eluting with 0–50% EtOAc in hexanes to afford 1,1,1,3,3,3-hexafluoro-2-(4-((2S)-2-(tetrahydro-2H-pyran-4-ylmethyl)-4-(2-thiophenylsulfonyl)-1-piperazinyl)phenyl)-2-propanol (20.0 mg, 4% yield) as a single enantiomer. <sup>1</sup>H NMR (400 MHz, CD<sub>3</sub>OD) δ = 7.92–7.87 (m, 1 H), 7.69–7.65 (m, 1 H), 7.56 (d, J = 8.8 Hz, 2 H), 7.31–7.24 (m, 1 H), 6.97 (d, J = 9.2 Hz, 2 H), 4.25–4.15 (m, 1 H), 3.96–3.84 (m, 2 H), 3.81–3.69 (m, 2 H), 3.60–3.52 (m, 1 H), 3.42–3.37 (m, 1 H), 3.31–3.27 (m, 1 H), 2.76–2.67 (m, 1 H), 2.64–2.52 (m, 1 H), 1.88–1.77 (m, 1 H), 1.76–1.68 (m, 1 H), 1.63–1.39 (m, 3 H), 1.33–1.12 (m, 3 H). *m/z* (ESI, +ve ion) 572.9 (M + H)<sup>+</sup>.

**1,1,1,3,3,3-Hexafluoro-2-(4-((2S)-2-(4-morpholinylmethyl)-4-(2-thiophenylsulfonyl)-1-piperazinyl)phenyl)-2-propanol (19).** Using morpholine and following the procedure given for compound 20 gave the desired product 1,1,1,3,3,3-hexafluoro-2-(4-((2S)-2-(4-morpholinylmethyl)-4-(2-thiophenylsulfonyl)-1-piperazinyl)phenyl)-2-propanol (60.0 mg, 3% yield over five steps) after purification by silica gel chromatography, eluting with 0–100% EtOAc in hexanes. <sup>1</sup>H NMR (400 MHz, CD<sub>3</sub>OD) δ = 7.87 (dd, J = 1.2, 5.1 Hz, 1 H), 7.64 (dd, J = 1.4, 3.7 Hz, 1 H), 7.53 (d, J = 8.8 Hz, 2 H), 7.25 (dd, J = 3.8, 5.0 Hz, 1 H), 6.95 (d, J = 9.2 Hz, 2 H), 4.17–4.09 (m, 1 H), 4.02–3.96 (m, 1 H), 3.82–3.75 (m, 1 H), 3.54 (t, J = 4.6 Hz, 5 H), 3.28–3.18 (m, 1 H), 2.80–2.70 (m, 1 H), 2.67–2.46 (m, 4 H), 2.40–2.25 (m, 3 H). *m/z* (ESI, +ve ion) 574.0 (M + H)<sup>+</sup>.

**1,1,1,3,3,3-Hexafluoro-2-(4-((2S)-2-(((3S)-3-methyl-4-morpholinyl)methyl)-4-(2-thiophenylsulfonyl)-1-piperazinyl)phenyl)-2-propanol (20).** A 2 L round-bottomed flask was charged with (S)-3-methylmorpholine (10.1 g, 100 mmol), HATU (39.7 g, 104 mmol), (R)-1,4-bis(*tert*-butoxycarbonyl)piperazine-2-carboxylic acid (30.0 g, 91 mmol), and 100 mL of DMF. To this was added Hünig's base (20.3 mL, 114 mmol). After stirring at room temperature for 1 h, the mixture was diluted with water (1 L) and then extracted with 750 mL of ether. The organic layer was separated and washed with water (4 × 500 mL), saturated aqueous NaHCO<sub>3</sub> (250 mL), brine (250 mL), dried with MgSO<sub>4</sub>, filtered, and concentrated to give (2R)-2-(((3S)-3-methyl-4-morpholinyl)carbonyl)-1,4-piperazinedicarboxylate (33.7 g, 90% yield) as a white solid.

A 1 L round-bottomed flask was charged with ((2R)-2-(((3S)-3-methyl-4-morpholinyl)carbonyl)-1,4-piperazinedicarboxylate (33.7 g, 82.0 mmol) and 100 mL of THF. To this was added borane–THF complex (1 M in THF, 327 mL, 327 mmol). The mixture was warmed to 50 °C for 2 h, then cooled to 0 °C and slowly quenched with 100 mL of MeOH. The mixture was concentrated in vacuo and then diluted with 200 mL of EtOAc. To this was added 100 mL of 4N HCl in dioxane. The mixture was heated at 70 °C for 2.5 h, and the resulting white precipitate was collected by filtration to give the amine tris-HCl salt. This solid was suspended in 200 mL of CH<sub>2</sub>Cl<sub>2</sub> and triethylamine (57.0 mL, 408 mmol). After cooling to 0 °C, 2-thiophenylsulfonyl chloride (14.9 g, 82.0 mmol) was added. The mixture was stirred at room temperature for 1 h and then diluted with water and extracted with EtOAc. The combined organics were dried (MgSO<sub>4</sub>), filtered, and concentrated to give an oil. Purification by silica gel chromatography eluting with 0–10% MeOH in CH<sub>2</sub>Cl<sub>2</sub> to afford (3S)-3-methyl-4-(((2S)-4-(2-thiophenylsulfonyl)-2-piperazinyl)methyl)morpholine (20.2 g, 71% yield) as a white solid. <sup>1</sup>H NMR (400 MHz, CD<sub>3</sub>OD) δ = 7.86 (dd, J = 1.2, 4.9 Hz, 1 H), 7.60 (dd, J = 1.2, 3.7 Hz, 1 H), 7.24 (dd, J = 3.8, 5.0 Hz, 1 H), 3.78–3.70 (m, 2 H), 3.66 (d, J = 11.3 Hz, 2 H), 3.61–3.54 (m, 1 H), 3.29–3.23 (m, 1 H), 3.07–3.01 (m, 1 H), 2.92–2.83 (m, 2 H), 2.83–2.76 (m, 1 H), 2.72–2.63 (m, 1 H), 2.51–2.43 (m, 1 H), 2.43–2.37 (m, 1 H), 2.36–2.29 (m, 1 H), 2.09 (s, 2 H), 0.96 (d, J = 6.3 Hz, 3 H).

The free base from the previous step was taken up in ether and acidified with 4N HCl in dioxane (2 mL, 8 mmol), and the resulting precipitate was collected to give the bis HCl salt as a white powder. In a pressure tube (3S)-3-methyl-4-(((2S)-4-(2-thiophenylsulfonyl)-2-piperazinyl)methyl)morpholine dihydrochloride (133 mg, 0.318 mmol), 2-(4-bromophenyl)-1,1,1,3,3,3-hexafluoropropan-2-ol (123

mg, 0.381 mmol), tris(dibenzylideneacetone)dipalladium (0) (18.3 mg, 0.032 mmol), dicyclohexyl(2',6'-diisopropoxybiphenyl-2-yl)-phosphine (RuPhos) (14.8 mg, 0.032 mmol), and sodium *tert*-butoxide (122 mg, 1.27 mmol) were combined and suspended in toluene (5 mL). Nitrogen gas was bubbled through the solution for 5 min. The reaction vial was sealed and heated to 100 °C for 15 h. The reaction mixture was then diluted with water and EtOAc. The aqueous mixture was extracted with EtOAc (2 × 20 mL). The organic extracts were combined and dried over MgSO<sub>4</sub>, filtered, and concentrated. The crude material was purified by purified via reverse-phase preparative HPLC using a Phenomenex Gemini C<sub>18</sub> column (30 mm × 150 mm, 10 μm) eluting with 0.1% TFA in MeCN/H<sub>2</sub>O (10% to 100% over 15 min) to afford 1,1,1,3,3,3-hexafluoro-2-(4-((2S)-2-(((3S)-3-methyl-4-morpholinyl)methyl)-4-(2-thiophenylsulfonyl)-1-piperazinyl)phenyl)-2-propanol (23.0 mg, 12% yield). <sup>1</sup>H NMR (400 MHz, CDCl<sub>3</sub>) δ 7.65 (d, J = 4.9 Hz, 1 H), 7.59 (m, 1 H), 7.54 (d, J = 8.8 Hz, 2 H), 7.17 (m, 1 H), 6.83 (d, J = 9.0 Hz, 2 H), 4.10 (m, 1 H), 3.91 (m, 1 H), 3.81 (m, 1 H), 3.69 (m, 1 H), 3.58 (m, 2 H), 3.46 (m, 1 H), 3.25 (m, 3 H), 2.75 (m, 1 H), 2.54 (m, 2 H), 2.39 (m, 1 H), 2.21 (m, 1 H), 1.97 (m, 1 H), 1.03 (d, J = 6.3 Hz, 3 H). *m/z* (ESI, +ve ion) 588.6 (M + H)<sup>+</sup>.

**Procedure for the Preparation of Chiral 2-(4-Bromophenyl)-1,1,1-trifluoro-2-propanol.** A 500 mL round-bottomed flask was charged with 1,4-dibromobenzene (30.3 g, 128 mmol) and 200 mL of diethylether. After cooling to –78 °C, *n*-BuLi (2.5 M in hexanes, 59.0 mL, 148 mmol) was added. This mixture was stirred for 15 min at –78 °C, then 1,1,1-trifluoro-2-propanone (30.5 g, 24.2 mL, 257 mmol) was added. Stirring was continued at –78 °C for 30 min, and then the reaction was quenched with 100 mL of saturated aqueous NH<sub>4</sub>Cl. The mixture was allowed to warm to rt and extracted with EtOAc (250 mL), dried (MgSO<sub>4</sub>), filtered, and concentrated to give an oil. Purification via silica gel chromatography (0–30% EtOAc in hexanes) gave 2-(4-bromophenyl)-1,1,1-trifluoro-2-propanol (21.5 g, 64%) as a colorless oil. The individual isomers were isolated using chiral SFC (Chiralcel OJH column (250 mm × 30 mm, 50 μm) with 5% 2-propanol in supercritical CO<sub>2</sub> (total flow was 120 mL/min)) to give both the *R* and *S* isomers with enantiomeric excesses >95%. The first eluting peak was assigned as the *R* isomer based on literature precedent.<sup>39</sup>

**(2R)-1,1,1-Trifluoro-2-(4-((2S)-2-(tetrahydro-2H-pyran-4-ylmethyl)-4-(2-thiophenylsulfonyl)-1-piperazinyl)phenyl)-2-propanol (23).** Using (3S)-3-(tetrahydro-2H-pyran-4-ylmethyl)-1-(2-thiophenylsulfonyl)piperazine (from compound 18 experimental) and following the procedure for compound 25 using (2R)-2-(4-bromophenyl)-1,1,1-trifluoro-2-propanol gave the desired product (2R)-1,1,1-trifluoro-2-(4-((2S)-2-(tetrahydro-2H-pyran-4-ylmethyl)-4-(2-thiophenylsulfonyl)-1-piperazinyl)phenyl)-2-propanol (5.00 mg, 1% yield) after purification by silica gel chromatography, eluting with 0–50% EtOAc in hexanes. <sup>1</sup>H NMR (400 MHz, CD<sub>3</sub>OD) δ = 7.86 (dd, J = 1.2, 5.1 Hz, 1 H), 7.63 (dd, J = 1.2, 3.9 Hz, 1 H), 7.44 (d, J = 8.8 Hz, 2 H), 7.24 (dd, J = 3.8, 5.0 Hz, 1 H), 6.89 (d, J = 8.8 Hz, 2 H), 4.12–4.04 (m, 1 H), 3.91–3.80 (m, 2 H), 3.75–3.61 (m, 2 H), 3.48–3.41 (m, 1 H), 3.38–3.33 (m, 1 H), 3.28–3.21 (m, 1 H), 2.77–2.66 (m, 1 H), 2.64–2.50 (m, 1 H), 1.80–1.69 (m, 2 H), 1.67 (s, 3 H), 1.59–1.43 (m, 2 H), 1.41–1.28 (m, 2 H), 1.27–1.06 (m, 2 H). *m/z* (ESI, +ve ion) 518.9 (M + H)<sup>+</sup>.

**(2S)-1,1,1-Trifluoro-2-(4-((2S)-2-(tetrahydro-2H-pyran-4-ylmethyl)-4-(2-thiophenylsulfonyl)-1-piperazinyl)phenyl)-2-propanol (24).** Using (3S)-3-(tetrahydro-2H-pyran-4-ylmethyl)-1-(2-thiophenylsulfonyl)piperazine (from compound 18 experimental) and following the procedure for compound 25 using (2S)-2-(4-bromophenyl)-1,1,1-trifluoro-2-propanol gave the desired product (2S)-1,1,1-trifluoro-2-(4-((2S)-2-(tetrahydro-2H-pyran-4-ylmethyl)-4-(2-thiophenylsulfonyl)-1-piperazinyl)phenyl)-2-propanol (10.0 mg, 2% yield) after purification by silica gel chromatography, eluting with 0–50% EtOAc in hexanes. <sup>1</sup>H NMR (400 MHz, CD<sub>3</sub>OD) δ = 7.87 (dd, J = 1.3, 5.0 Hz, 1 H), 7.64 (dd, J = 1.4, 3.7 Hz, 1 H), 7.45 (d, J = 8.8 Hz, 2 H), 7.25 (dd, J = 3.8, 5.0 Hz, 1 H), 6.90 (d, J = 9.0 Hz, 2 H), 4.12–4.06 (m, 1 H), 3.91–3.81 (m, 2 H), 3.76–3.63 (m, 2 H), 3.48–3.42 (m, 1 H), 3.39–3.34 (m, 1 H), 3.29–3.23 (m, 1 H), 2.75–2.69 (m, 1 H), 2.59 (dt, J = 3.7, 11.4 Hz, 1 H), 1.81–1.73 (m, 2 H),

1.68 (s, 3 H), 1.60–1.44 (m, 2 H), 1.42–1.27 (m, 2 H), 1.28–1.07 (m, 2 H).  $m/z$  (ESI, +ve ion) 519.0 (M + H)<sup>+</sup>.

(2R)-1,1,1-Trifluoro-2-(4-((2S)-2-(((3S)-3-methyl-4-morpholinyl)-methyl)-4-(2-thiophenylsulfonyl)-1-piperazinyl)phenyl)-2-propanol (**25**, AMG-1694). A 1 L pressure vessel was charged with (S)-3-methyl-4-(((S)-4-(thiophen-2-ylsulfonyl)piperazin-2-yl)methyl)morpholine (from compound **20** experimental, 10.5 g, 30.4 mmol), 100 mL of toluene, (R)-2-(4-bromophenyl)-1,1,1-trifluoropropan-2-ol (9.81 g, 36.5 mmol), and sodium 2-methylpropan-2-olate (7.30 g, 76.0 mmol). This mixture was degassed (by bubbling nitrogen gas through the solution for 3 min) then chloro(2-dicyclohexylphosphino-2',6'-diisopropoxy-1,1'-biphenyl)[2-(2-aminoethylphenyl)]palladium(II), methyl-*tert*-butylether adduct (RuPhos first generation precatalyst) (1.11 g, 1.52 mmol), and dicyclohexyl(2',6'-diisopropoxy-[1,1'-biphenyl]-2-yl)phosphine (RuPhos) (0.709 g, 1.52 mmol) were added. The vessel was sealed and heated at 60 °C for 12 h. The mixture diluted with water and extracted with EtOAc, and the combined organics were dried with MgSO<sub>4</sub>, filtered, concentrated, and purified by silica gel chromatography eluting with 0–70% ethyl acetate in hexanes to give (R)-1,1,1-trifluoro-2-(4-((S)-2-(((S)-3-methylmorpholino)methyl)-4-(thiophen-2-ylsulfonyl)piperazin-1-yl)-phenyl)propan-2-ol (8.15 g, 50% yield) as a tan foam. <sup>1</sup>H NMR (400 MHz, CDCl<sub>3</sub>) δ 7.66–7.64 (dd,  $J$  = 5.1, 1.2 Hz, 1 H), 7.59–7.57 (dd,  $J$  = 3.7, 1.2 Hz, 1 H), 7.45–7.42 (d,  $J$  = 8.9 Hz, 2 H), 7.19–7.16 (m,  $J$  = 5.0, 3.7 Hz, 1 H), 6.82–6.80 (d,  $J$  = 8.9 Hz, 2 H), 4.09–4.04 (m, 1 H), 3.89–3.85 (m, 1 H), 3.80–3.75 (m, 1 H), 3.73–3.69 (m, 1 H), 3.65–3.54 (m, 2 H), 3.43–3.38 (m, 1 H), 3.30–3.20 (m, 3 H), 2.76–2.71 (m, 1 H), 2.62–2.50 (m, 2 H), 2.40–2.34 (m, 1 H), 2.21–2.14 (m, 1 H), 1.94–1.89 (m, 1 H), 1.74 (s, 3 H), 1.03–1.02 (d,  $J$  = 6.1 Hz, 3 H).  $m/z$  (ESI, +ve ion) 533.9 (M + H)<sup>+</sup>.

(2S)-1,1,1-Trifluoro-2-(4-((2S)-2-(((3S)-3-methyl-4-morpholinyl)-methyl)-4-(2-thiophenylsulfonyl)-1-piperazinyl)phenyl)-2-propanol (**26**). Following the procedure for compound **25** using (2S)-2-(4-bromophenyl)-1,1,1-trifluoro-2-propanol gave the desired product (2S)-1,1,1-trifluoro-2-(4-((2S)-2-(((3S)-3-methyl-4-morpholinyl)-methyl)-4-(2-thiophenylsulfonyl)-1-piperazinyl)phenyl)-2-propanol (32.4 mg, 70% yield). <sup>1</sup>H NMR (400 MHz, CDCl<sub>3</sub>) δ 7.66–7.64 (dd,  $J$  = 5.1, 1.2 Hz, 1 H), 7.59–7.57 (dd,  $J$  = 3.7, 1.2 Hz, 1 H), 7.45–7.42 (d,  $J$  = 8.9 Hz, 2 H), 7.19–7.16 (m,  $J$  = 5.0, 3.7 Hz, 1 H), 6.82–6.80 (d,  $J$  = 8.9 Hz, 2 H), 4.09–4.04 (m, 1 H), 3.89–3.85 (m, 1 H), 3.80–3.75 (m, 1 H), 3.73–3.69 (m, 1 H), 3.65–3.54 (m, 2 H), 3.43–3.38 (m, 1 H), 3.30–3.20 (m, 3 H), 2.76–2.71 (m, 1 H), 2.62–2.50 (m, 2 H), 2.40–2.34 (m, 1 H), 2.21–2.14 (m, 1 H), 1.94–1.89 (m, 1 H), 1.74 (s, 3 H), 1.03–1.02 (d,  $J$  = 6.1 Hz, 3 H).  $m/z$  (ESI, +ve ion) 534.2 (M + H)<sup>+</sup>.

## ■ ASSOCIATED CONTENT

### Supporting Information

Standard deviation for the in vitro activities listed in Tables 1, 2 and 4. This material is available free of charge via the Internet at <http://pubs.acs.org>. For 4MSU, The Advanced Light Source is supported by the U.S. Department of Energy under contract no. DE-AC02-05CH11231.

### Accession Codes

PDB ID codes for **1** and **25** bound to hGKRP are 4MSU and 4LY9, respectively.

## ■ AUTHOR INFORMATION

### Corresponding Author

\*Phone: 805-313-5532. E-mail: [katea@amgen.com](mailto:katea@amgen.com).

### Present Addresses

▽Genentech, Inc., One DNA Way, South San Francisco, California 94080-4990, United States.

○Division of Comparative Medicine, Beckman Research Institute, City of Hope, 1500 East Duarte Road, Duarte, California 91010-3000, United States.

◆JD Consulting, 1969 Roadrunner Avenue, Thousand Oaks, California 91360-6560, United States.

### Notes

The authors declare the following competing financial interest(s): The authors declare competing financial interests as employees of Amgen Inc..

## ■ ACKNOWLEDGMENTS

We acknowledge Kyung Gahm, Wesley Barnhart, and Samuel Thomas for conducting the SFC separations and Mark Norman and Mike Bartberger for their input on the preparation of this manuscript. Additionally, we thank Scott Simonet, Murielle Véniant, Philip Tagari, and Randall Hungate for their support of this research.

## ■ ABBREVIATIONS USED

Alpha, amplified luminescent proximity assay; DMEM, Dulbecco's Modified Eagle Medium;  $f_w$ , fraction unbound; G6P, glucose-6-phosphate; GK, glucokinase; GKA, glucokinase activator; GKRP, glucokinase regulatory protein; HTS, high throughput screen; IHC, immunohistochemistry; RuPhos, dicyclohexyl(2',6'-diisopropoxybiphenyl-2-yl)phosphine; RuPhos first-generation precatalyst, chloro(2-dicyclohexylphosphino-2',6'-diisopropoxy-1,1'-biphenyl)[2-(2-aminoethyl)phenyl]-palladium(II) methyl-*t*-butyl ether adduct; S6P, D-sorbitol-6-phosphate; SPR, surface plasmon resonance; ZDF, Zucker diabetic fatty

## ■ REFERENCES

- (1) Agius, L. Glucokinase and Molecular Aspects of Liver Glycogen Metabolism. *Biochem. J.* **2008**, *414*, 1–18.
- (2) Matschinsky, F. M.; Liang, Y.; Kesavan, P.; Wang, L.; Froguel, P.; Velho, G.; Cohen, D.; Permutt, M. A.; Tanizawa, Y.; Jetton, T. L.; Niswender, K.; Magnuson, M. Glucokinase as a Glucose Sensor and Metabolic Signal Generator in Pancreatic Beta-Cells and Hepatocytes. *Hepatology* **1990**, *39* (6), 647–652.
- (3) Coghlan, M.; Leighton, B. Glucokinase Activators in Diabetes Management. *Expert Opin. Invest. Drugs* **2008**, *17* (2), 145–167.
- (4) Grimsby, J.; Berthel, S. J.; Sarabu, R. Glucokinase Activators for the Potential Treatment of Type 2 Diabetes. *Curr. Top. Med. Chem.* **2008**, *8* (17), 1524–1532.
- (5) Fyfe, M. C. T.; Procter, M. J. Glucokinase Activators as Potential Antidiabetic Agents Possessing Superior Glucose Lowering Efficacies. *Drugs Future* **2009**, *34* (8), 641–654.
- (6) Meininger, G. E.; Scott, R.; Alba, M.; Shentu, Y.; Luo, E.; Amin, H.; Davies, M. J.; Kaufman, K. D.; Goldstein, B. J. Effects of MK-0941, a Novel Glucokinase Activator, on Glycemic Control in Insulin-Treated Patients with Type 2 Diabetes. *Diabetes Care* **2011**, *34* (12), 2560–2566.
- (7) Matschinsky, F. M.; Zelent, B.; Doliba, N.; Changhong, L.; Vanderkooi, J. M.; Naji, A.; Sarabu, R.; Grimsby, J. Glucokinase Activators for Diabetes Therapy (May 2010 status report). *Diabetes Care* **2011**, *34* (Suppl 2), S236–S243.
- (8) Rees, M. G.; Gloyn, A. L. Small Molecular Glucokinase Activators: Has Another New Anti-Diabetic Therapeutic Lost Favour? *Br. J. Pharmacol.* **2013**, *168* (2), 335–8.
- (9) Matschinsky, F. M. GKAs for Diabetes Therapy: Why No Clinically Useful Drug After Two Decades of Trying? *Trends Pharmacol. Sci.* **2013**, *34* (2), 90–99.
- (10) Human genetic data indicates that loss of function of glucokinase results in hyperglycemia and associated conditions: Gloyn, A. L. Glucokinase (GCK) Mutations in Hyper- and Hypoglycemia: Maturity-Onset Diabetes of the Young, Permanent Neonatal Diabetes, and Hyperinsulinemia of Infancy. *Hum. Mutat.* **2003**, *22* (5), 353–362.

- (11) Farrelly, D.; Brown, K. S.; Tieman, A.; Ren, J.; Lira, S. A.; Hagan, D.; Gregg, R.; Mookhtiar, K. A.; Hariharan, N. Mice Mutant for Glucokinase Regulatory Protein Exhibit Decreased Liver Glucokinase: A Sequestration Mechanism in Metabolic Regulation. *Proc. Natl. Acad. Sci. U. S. A.* **1999**, *96* (25), 14511–14516.
- (12) Vandercammen, A.; Van Schaftingen, E. The Mechanism by Which Rat Liver Glucokinase is Inhibited by the Regulatory Protein. *Eur. J. Biochem.* **1990**, *191* (2), 483–489.
- (13) Van Schaftingen, E.; Vandercammen, A.; Detheux, M.; Davies, D. R. The Regulatory Protein of Liver Glucokinase. *Adv. Enzyme Regul.* **1992**, *32*, 133–148.
- (14) Anderka, O.; Boyken, J.; Aschenbach, U.; Batzer, A.; Boscheinen, O.; Schmoll, D. Biophysical Characterization of the Interaction Between Hepatic Glucokinase and its Regulatory Protein: Impact of Physiological and Pharmacological Effectors. *J. Biol. Chem.* **2008**, *283* (46), 31333–31340.
- (15) Van Schaftingen, E.; Viegas da Cunha, M. Discovery and Role of Glucokinase Regulatory Protein. *Glucokinase and Glycemic Diseases: From Basics to Novel Therapeutics*; Frontiers in Diabetes, Vol. 16; Matschinsky, F. M.; Magnuson, M. A.; Belfiore, F., Eds.; S. Karger AG: Basel, Switzerland, 2004, pp 193–208.
- (16) Pfeifferkorn, J. A. Strategies for the Design of Hepatoselective Glucokinase Activators to Treat Type 2 Diabetes. *Expert Opin. Drug Discovery* **2013**, *8* (3), 319–330.
- (17) Chen, K.; Michelsen, K.; Kurzeja, R.; Han, J.; Mukta, V.; St. Jean, D. J., Jr.; Hale, C.; Wahl, R. Unpublished results.
- (18) Wolff, M.; Kauschke, S. G.; Schmidt, S.; Heilker, R. Activation and Translocation of Glucokinase in Rat Primary Hepatocytes Monitored by High Content Image Analysis. *J. Biomol. Screening* **2008**, *13* (9), 837–846.
- (19) The interaction with GKRP was confirmed via surface plasmon resonance (SPR) analysis ( $K_D$  of 0.24  $\mu$ M). This compound did not interact with GK. The  $EC_{50}$  of **1** in a hGK dose response was >50  $\mu$ M.
- (20) Pautsch, A.; Stadler, N.; Lohle, A.; Rist, W.; Berg, A.; Glocker, L.; Nar, H.; Reinert, D.; Lenter, M.; Heckel, A.; Schnapp, G.; Kauschke, S. G. Crystal Structure of Glucokinase Regulatory Protein. *Biochemistry* **2013**, *52* (20), 3523–3531.
- (21) Choi, J. M.; Seo, M.-H.; Kyeong, H.-H.; Kim, E.; Kim, H.-S. Molecular Basis for the Role of Glucokinase Regulatory Protein as the Allosteric Switch for Glucokinase. *Proc. Natl. Acad. Sci. U. S. A.* **2013**, *110* (25), 10171–10176.
- (22) Lloyd, D. J.; St. Jean, D. J.; Kurzeja, R. J. M.; Wahl, R. C.; Michelsen, K.; Cupples, R.; Chen, M.; Wu, J.; Sivits, G.; Helmering, J.; Ashton, K. S.; Pennington, L. D.; Fotsch, C. H.; Vazir, M.; Chen, K.; Chmait, S.; Zhang, J.; Liu, L.; Norman, M. H.; Andrews, K. A.; Bartberger, M. D.; Van, G.; Galbreath, E. J.; Vonderfecht, S. L.; Wang, M.; Jordan, S. R.; Véniant, M. M.; Hale, C. Anti-Diabetic Effects of a Glucokinase Regulatory Protein Small Molecule Disruptor. *Nature* **2013**, *504*, 437–440.
- (23) BE calculated based upon the  $K_D$  value of 0.24  $\mu$ M. Kuntz, I. D.; Chen, K.; Sharp, K. A.; Kollman, P. A. *Proc. Natl. Acad. Sci. U. S. A.* **1999**, *96* (18), 9997–10002.
- (24) (a) Johnson, F. Allylic strain in six-membered rings. *Chem. Rev.* **1968**, *68* (4), 375–413. (b) Quantum mechanical calculations on the model system (S)-2-methyl-4-(methylsulfonyl)-1-phenylpiperazine were performed using B3LYP/6-31G\* in Gaussian 03. Frisch, M. J.; Trucks, G. W.; Schlegel, H. B.; Scuseria, G. E.; Robb, M. A.; Cheeseman, J. R.; Montgomery, Jr., J. A.; Vreven, T.; Kudin, K. N.; Burant, J. C.; Millam, J. M.; Iyengar, S. S.; Tomasi, J.; Barone, V.; Mennucci, B.; Cossi, M.; Scalmani, G.; Rega, N.; Petersson, G. A.; Nakatsuji, H.; Hada, M.; Ehara, M.; Toyota, K.; Fukuda, R.; Hasegawa, J.; Ishida, M.; Nakajima, T.; Honda, Y.; Kitao, O.; Nakai, H.; Klene, M.; Li, X.; Knox, J. E.; Hratchian, H. P.; Cross, J. B.; Bakken, V.; Adamo, C.; Jaramillo, J.; Gomperts, R.; Stratmann, R. E.; Yazyev, O.; Austin, A. J.; Cammi, R.; Pomelli, C.; Ochterski, J. W.; Ayala, P. Y.; Morokuma, K.; Voth, G. A.; Salvador, P.; Dannenberg, J. J.; Zakrzewski, V. G.; Dapprich, S.; Daniels, A. D.; Strain, M. C.; Farkas, O.; Malick, D. K.; Rabuck, A. D.; Raghavachari, K.; Foresman, J. B.; Ortiz, J. V.; Cui, Q.; Baboul, A. G.; Clifford, S.; Cioslowski, J.; Stefanov, B. B.; Liu, G.; Liashenko, A.; Piskorz, P.; Komaromi, I.; Martin, R. L.; Fox, D. J.; Keith, T.; Al-Laham, M. A.; Peng, C. Y.; Nanayakkara, A.; Challacombe, M.; Gill, P. M. W.; Johnson, B.; Chen, W.; Wong, M. W.; Gonzalez, C.; Pople, J. A. *Gaussian 03*, revision C.02; Gaussian, Inc.: Wallingford CT, 2004. The axial (S)-Me conformation was preferred by 1.25 kcal over the equatorial. In addition, the equatorial low energy conformation twists the phenyl ring  $\sim 34^\circ$  compared to the axial conformation which would also impact binding to GKRP.
- (25) Given the poor PK within this class of compounds, and in order to keep the dose below 100 mg/kg, we rationalized that a compound with cellular activity of 100 nM or better was required to allow for target coverage in vivo.
- (26) Quantum mechanical calculations on the model system (S)-4-ethyl-3-methylmorpholine using B3LYP/6-31G\* in Gaussian 03 Frisch, M. J.; Trucks, G. W.; Schlegel, H. B.; Scuseria, G. E.; Robb, M. A.; Cheeseman, J. R.; Montgomery, Jr., J. A.; Vreven, T.; Kudin, K. N.; Burant, J. C.; Millam, J. M.; Iyengar, S. S.; Tomasi, J.; Barone, V.; Mennucci, B.; Cossi, M.; Scalmani, G.; Rega, N.; Petersson, G. A.; Nakatsuji, H.; Hada, M.; Ehara, M.; Toyota, K.; Fukuda, R.; Hasegawa, J.; Ishida, M.; Nakajima, T.; Honda, Y.; Kitao, O.; Nakai, H.; Klene, M.; Li, X.; Knox, J. E.; Hratchian, H. P.; Cross, J. B.; Bakken, V.; Adamo, C.; Jaramillo, J.; Gomperts, R.; Stratmann, R. E.; Yazyev, O.; Austin, A. J.; Cammi, R.; Pomelli, C.; Ochterski, J. W.; Ayala, P. Y.; Morokuma, K.; Voth, G. A.; Salvador, P.; Dannenberg, J. J.; Zakrzewski, V. G.; Dapprich, S.; Daniels, A. D.; Strain, M. C.; Farkas, O.; Malick, D. K.; Rabuck, A. D.; Raghavachari, K.; Foresman, J. B.; Ortiz, J. V.; Cui, Q.; Baboul, A. G.; Clifford, S.; Cioslowski, J.; Stefanov, B. B.; Liu, G.; Liashenko, A.; Piskorz, P.; Komaromi, I.; Martin, R. L.; Fox, D. J.; Keith, T.; Al-Laham, M. A.; Peng, C. Y.; Nanayakkara, A.; Challacombe, M.; Gill, P. M. W.; Johnson, B.; Chen, W.; Wong, M. W.; Gonzalez, C.; and Pople, J. A.; *Gaussian 03*, revision C.02; Gaussian, Inc.: Wallingford CT, 2004 showed that the (S)-Me substituent preferred to be axial by 1.9 kcal.
- (27) Leeson, P. D.; Springthorpe, B. The Influence of Drug-Like Concepts on Decision-Making in Medicinal Chemistry. *Nature Rev. Drug Discovery* **2007**, *6*, 881–890.
- (28) Following a 100 mg/kg oral dose of **25** to Wistar rats, the unbound  $C_{max}$  was 0.056  $\mu$ M.
- (29) Ashton, K. S.; Denti, M.; Norman, M. H.; St. Jean Jr., D. J. Unpublished results.
- (30) Bourbeau, M.; Ashton, K. S.; St. Jean Jr., D. J. Unpublished results.
- (31) Shin, J.-S.; Torres, T. P.; Catlin, R. L.; Donahue, E. P.; Shiota, M. A defect in glucose-induced dissociation of glucokinase from the regulatory protein in Zucker diabetic fatty rats in the early stages of diabetes. *Am. J. Physiol.: Regul. Integr. Comp. Physiol.* **2007**, *292*, 1381–1390.
- (32) For a 30 mg/kg oral dose of compound **25** at the 1 h time point, the portal vein concentration:jugular vein concentration is 3:1 (unpublished results).
- (33) Glucose:fructose ratio is 2 g/kg:0.25 g/kg.
- (34) Grimsby, J.; Sarabu, R.; Corbett, W. L.; Haynes, N.-E.; Bizzarro, F. T.; Coffey, J. W.; Guertin, K. R.; Hilliard, D. W.; Kester, R. F.; Mahaney, P. E.; Marcus, L.; Qi, L.; Spence, C. L.; Teng, J.; Magnuson, M.; An Chu, C.; Dvorozniak, M. T.; Matschinsky, F. M.; Grippo, J. F. Allosteric Activators of Glucokinase: Potential Role in Diabetes Therapy. *Science* **2003**, *301* (5631), 370–373.
- (35) The  $EC_{50}$  of **25** in a hGK dose response was >50  $\mu$ M.
- (36) St. Jean, D. J.; Ashton, K. S.; Bartberger, M. D.; Chen, J.; Chmait, S.; Cupples, R.; Galbreath, E.; Helmering, J.; Hong, F.-T.; Jordan, S. R.; Liu, L.; Kunz, R. K.; Michelsen, K.; Nishimura, N.; Pennington, L. D.; Poon, S. F.; Reid, D.; Sivits, G.; Stec, M. M.; Tadesse, S.; Tamayo, N.; Van, G.; Yang, K.; Zhang, J.; Norman, M. H.; Fotsch, C.; Lloyd, D. J.; Hale, C. Small Molecule Disruptors of the Glucokinase–Glucokinase Regulatory Protein Interaction: 2. Leveraging Structure-Based Drug Design to Identify Analogs with Improved Pharmacokinetic Profiles. *J. Med. Chem.* **2014**, DOI: 10.1021/jm4016747.



(37) Kreamer, B. L.; Staecker, J. L.; Sawada, N.; Sattler, G. L.; Hsia, M. T. S.; Pitot, H. C. Use of a Low-speed, Iso-density Percoll Centrifugation Method to Increase the Viability of Isolated Rat Hepatocyte Preparations. *In Vitro Cell Dev. Biol.* **1986**, 22 (4), 201–211.

(38) Frenette, R.; Blouin, M.; Brideau, C.; Chauret, N.; Ducharme, Y.; Friesen, R. W.; Hamel, P.; Jones, T. R.; Laliberté, F.; Li, C.; Masson, P.; McAuliffe, M.; Girard, Y. Substituted 4-(2,2-diphenylethyl)pyridine-*N*-oxides as Phosphodiesterase-4 Inhibitors: SAR Study Directed Toward the Improvement of Pharmacokinetic Parameters. *Bioorg. Med. Chem. Lett.* **2002**, 12 (20), 3009–3013.

(39) Mizuta, S.; Shibata, N.; Akiti, S.; Fujimoto, H.; Nakamura, S.; Toru, T. Cinchona Alkaloid-Catalyzed Asymmetric Trifluoromethylation of Alkynyl Ketones with Trimethylsilyl Trifluoromethane. *Org. Lett.* **2007**, 9 (18), 3707–3710.